Agricultural and Forest Meteorology 197 (2014) 142–157

Contents lists available at ScienceDirect

Agricultural and Forest Meteorology

journal homepage: www.elsevier.com/locate/agrformet

Data-driven diagnostics of terrestrial carbon dynamics over North America

Jingfeng Xiao[a,*], Scott V. Ollinger[a], Steve Frolking[a], George C. Hurtt[b], David Y. Hollinger[c], Kenneth J. Davis[d], Yude Pan[e], Xiaoyang Zhang[f], Feng Deng[g], Jiquan Chen[h], Dennis D. Baldocchi[i], Bevery E. Law[j], M. Altaf Arain[k], Ankur R. Desai[l], Andrew D. Richardson[m], Ge Sun[n], Brian Amiro[o], Hank Margolis[p], Lianhong Gu[q], Russell L. Scott[r], Peter D. Blanken[s], Andrew E. Suyker[t]

[a] Earth Systems Research Center, Institute for the Study of Earth, Oceans, and Space, University of New Hampshire, Durham, NH 03824, USA
[b] Center for Global Change & Earth Observations, Department of Geography, Michigan State University, East Lansing, MI 48823, USA
[c] USDA Forest Service, Northern Research Station, Durham, NH 03824, USA
[d] Department of Meteorology, Pennsylvania State University, University Park, PA 16802, USA
[e] U.S. Department of Agriculture Forest Service, Newtown Square, PA 19073, USA
[f] Geospatial Sciences Center of Excellence, South Dakota State University, Brookings, SD 57007, USA
[g] Department of Physics, University of Toronto, Canada
[h] Department of Environmental Sciences, University of Toledo, Toledo, OH 43606, USA
[i] Ecosystem Science Division, Department of Environmental Science, Policy and Management, University of California, Berkeley, CA 94720, USA
[j] Department of Forest Ecosystems and Society, Oregon State University, Corvallis, OR 97331, USA
[k] McMaster Centre for Climate Change and School of Geography and Earth Sciences, McMaster University, Hamilton, Ontario, Canada
[l] Department of Atmospheric & Oceanic Sciences, University of Wisconsin, Madison, WI 53706, USA
[m] Department of Organismic and Evolutionary Biology, Harvard University, Cambridge, MA 02138, USA
[n] Eastern Forest Environmental Threat Assessment Center, Southern Research Station, USDA Forest Service, Raleigh, NC 27606, USA
[o] Department of Soil Science, University of Manitoba, Winnipeg, Manitoba, Canada
[p] Centre d'Étude de la Forêt, Faculté de Foresterie, de Géographie et de Géomatique, Université Laval, Québec G1V 0A6, Canada
[q] Environmental Sciences Division, Oak Ridge National Laboratory, Oak Ridge, TN 37831, USA
[r] USDA-ARS Southwest Watershed Research Center, Tucson, AZ 85719, USA
[s] Department of Geography, University of Colorado at Boulder, Boulder, CO 80309, USA
[t] School of Natural Resources, University of Nebraska-Lincoln, Lincoln, NE 68583, USA

ARTICLE INFO

Article history:
Received 2 April 2014
Received in revised form 23 June 2014
Accepted 29 June 2014

Keywords:
Carbon sink
Carbon source
Disturbance
Eddy covariance
Drought
EVI

ABSTRACT

The exchange of carbon dioxide is a key measure of ecosystem metabolism and a critical intersection between the terrestrial biosphere and the Earth's climate. Despite the general agreement that the terrestrial ecosystems in North America provide a sizeable carbon sink, the size and distribution of the sink remain uncertain. We use a data-driven approach to upscale eddy covariance flux observations from towers to the continental scale by integrating flux observations, meteorology, stand age, aboveground biomass, and a proxy for canopy nitrogen concentrations from AmeriFlux and Fluxnet-Canada Research Network as well as a variety of satellite data streams from the MODIS sensors. We then use the resulting gridded flux estimates from March 2000 to December 2012 to assess the magnitude, distribution, and interannual variability of carbon fluxes for the U.S. and Canada. The mean annual gross primary productivity (GPP), ecosystem respiration (ER), and net ecosystem productivity (NEP) of the U.S. over the period 2001–2012 were 6.84, 5.31, and 1.10 Pg C yr^{-1}, respectively; the mean annual GPP, ER, and NEP of Canada over the same 12-year period were 3.91, 3.26, and 0.60 Pg C yr^{-1}, respectively. The mean nationwide annual NEP of natural ecosystems over the period 2001–2012 was 0.53 Pg C yr^{-1} for the U.S. and 0.49 Pg C yr^{-1} for the conterminous U.S. Our estimate of the carbon sink for the conterminous U.S. was almost identical with the estimate of the First State of the Carbon Cycle Report (SOCCR). The carbon fluxes exhibited relatively large interannual variability over the study period. The main sources of the interannual variability in carbon fluxes included drought and disturbance. The annual GPP and NEP were strongly related to annual evapotranspiration (ET) for both

* Corresponding author. Tel.: +1 603 862 1873; fax: +1 603 862 0188.
E-mail address: j.xiao@unh.edu (J. Xiao).

http://dx.doi.org/10.1016/j.agrformet.2014.06.013
0168-1923/© 2014 Elsevier B.V. All rights reserved.

the U.S. and Canada, showing that the carbon and water cycles were closely coupled. Our gridded flux estimates provided an independent, alternative perspective on ecosystem carbon exchange over North America.

© 2014 Elsevier B.V. All rights reserved.

1. Introduction

The net exchange of carbon dioxide (CO_2) is a key measure of ecosystem metabolism and a critical intersection between the terrestrial biosphere and the Earth's climate. Although there is general agreement that North American ecosystems provide a large carbon sink (Goodale et al., 2002; Gurney et al., 2002; Deng et al., 2007; Xiao et al., 2011a), the size and distribution of this sink are not well quantified and there are large uncertainties related to sources of variability over space and time. Extreme climate events (Ciais et al., 2005; Xiao et al., 2009; Zhao and Running, 2010) and disturbances such as fire (Bowman et al., 2009), hurricanes (Chambers et al., 2007; Xiao et al., 2011a), wind storms (McCarthy et al., 2006; Lindroth et al., 2009), and insect outbreaks (Kurz et al., 2008) can substantially alter ecosystem structure and function in ways that cause significant year-to-year variation in carbon budgets. In light of these factors, improved understanding of the variability in carbon dynamics over North America and quantification of associated uncertainties are essential for improving projections of the Earth's carbon-climate system under future climate conditions (IPCC, 2007).

To date, terrestrial carbon dynamics over North America have been most widely examined through use of ecosystem models (Schimel et al., 2000; Nemani et al., 2002) or inventory approaches (SOCCR, 2007; Pan et al., 2011a). The North American Carbon Program (NACP) Regional Interim Synthesis recently conducted a model intercomparison study and compared carbon simulations over North America over the period 2000–2005 from 22 ecosystem models. The model intercomparison showed that carbon fluxes exhibited enormous variability among these models for both spatial and temporal domains (Huntzinger et al., 2012; Raczka et al., 2013). This underscores the fact that, despite the substantial advances in ecosystem modeling, large uncertainties still exist in the spatial and temporal variability of carbon fluxes. Although inventory approaches can constrain this variability to some degree, these surveys capture only some of the relevant fluxes and at time scales that are too coarse for resolving important ecophysiological processes or their underlying drivers (Baldocchi et al., 2001).

In contrast, the eddy covariance (EC) technique provides an alternative approach to estimate net ecosystem exchange (NEE) through direct ecosystem-level measurements (Baldocchi et al., 2001; Baldocchi, 2008). NEE is routinely partitioned into gross primary productivity (GPP) and ecosystem respiration (ER). EC techniques provide quasi-continuous, high-frequency measurements of whole-ecosystem CO_2, water, and energy fluxes that can be used to examine ecosystem response to climate variability and disturbance over a range of time scales (Amiro et al., 2010; Schwalm et al., 2010). Tower-based estimates, however, sample an up-wind distance of a few kilometers, and thus represent a relatively small portion of the landscapes. These observations provide useful information over larger scales only when combined with rigorous methods of upscaling. To date, significant advances have been made in the upscaling of EC flux observations (Xiao et al., 2012). A number of studies have upscaled EC flux observations to large regions using satellite remote sensing data and modeling approaches (Xiao et al., 2008, 2010, 2011a,b; Jung et al., 2009; Ryu et al., 2011), and some of these studies have also used the resulting flux estimates to assess regional terrestrial carbon and water budgets (Sun et al., 2011; Xiao et al., 2010, 2011a,b; Zhang et al., 2014).

In our own work with the AmeriFlux network of flux measurement sites across the U.S. (Xiao et al., 2008, 2010, 2011a), we integrated EC flux data with satellite observations to produce continuous GPP and NEE estimates (as opposed to single annual snapshots) for the conterminous U.S., and assessed the magnitude, distribution, and interannual variability of the U.S. terrestrial carbon sink. Compared to inventory approaches and conventional ecological modeling, upscaling methods that explicitly integrate EC flux data and remote observations have the advantage of combining the high-temporal resolution afforded by towers with the broad spatial coverage provided by satellites (Xiao et al., 2008). The use of satellite data in this capacity is logical because remote platforms provide the only means of viewing large portions of the Earth's surface at regular intervals and the selective absorption and reflectance of light by plants allows orbital sensors to gather large amounts of information relevant to ecosystem functioning.

Despite the growing number of studies in upscaling EC flux observations, the effects of disturbance, stand age and nitrogen availability on ecosystem carbon dynamics have not been explicitly considered. Disturbance and stand age are important drivers of forest structure and function (Chapin et al., 2011), and are known to influence terrestrial carbon budgets (Liu et al., 2011; Deng et al., 2013). Similarly, the availability of nitrogen (N) is widely recognized as an important constraint on canopy photosynthesis (Field and Mooney, 1986; Wright et al., 2005) as well as whole-ecosystem carbon gain (Oren et al., 2001; Ainsworth and Long, 2005; Reich et al., 2006; Magnani et al., 2007; LeBauer and Treseder, 2008). In spite of growing scientific understanding of the roles of disturbance and canopy nitrogen in ecosystems, application to continental-scale analyses has lagged because of limited mapping of disturbance (Kennedy et al., 2010; Masek et al., 2013) and canopy nitrogen concentrations (Ollinger et al., 2008) over large regions.

In this study, we used EC flux observations from 94 sites across the U.S. and Canada, in combination with satellite data streams and new ecological data including stand age and aboveground biomass to generate gridded flux estimates for North America over the period 2000–2012. Our new flux estimates could partly account for the effects of disturbance and nitrogen limitation. The objectives of this study are: (1) to upscale flux observations from EC flux sites to the continental scale and to generate gridded flux estimates; (2) to examine the magnitude and spatial patterns of carbon fluxes; (3) to assess the interannual variability of carbon fluxes at the continental scale; and (4) to evaluate the responses of these fluxes to extreme climate events and large disturbance.

2. Data and methods

2.1. Flux observations

We used the EC flux observations from 68 sites in the U.S. and 26 sites in Canada (Fig. 1; See Supplementary Table S1). This network of EC sites across North America is broadly representative of environmental and climate space with the exception of the far northern (tundra) regions. Hargrove et al. (2003) conducted a multivariate analysis of environmental "data space" and concluded that the central, Midwestern, and northeastern U.S. were well represented

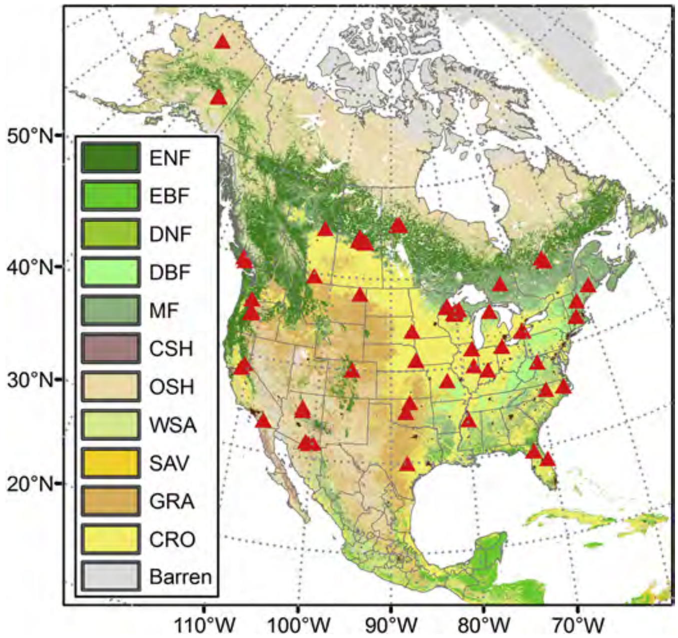

Fig. 1. Location and distribution of the eddy covariance flux sites from AmeriFlux and Fluxnet-Canada used in this study. The symbols stand for the locations of the sites. The base map is the 1 km-resolution land cover map derived from MODIS, and the vegetation types are evergreen needleleaf forests (ENF), evergreen broadleaf forests (EBF), deciduous needleleaf forests (DNF), deciduous broadleaf forests (DBF), mixed forests (MF), closed shrublands (CSH), open shrublands (OSH), woody savannas (WSA), savannas (SAV), grasslands (GRA), croplands (CRO).

by the AmeriFlux network, while the southern, southwestern, and Pacific Northwest regions were less well represented by the existing tower sites. Since that analysis, more than 20 new sites have been established in Florida, North Carolina, Texas, New Mexico, Arizona, and Southern California, which increased the spatial coverage and representativeness of the south and southwestern parts of the U.S. In addition, Hargrove et al. (2003) did not consider flux towers in Canada and Mexico. Including the ~20 flux towers that comprised the Fluxnet-Canada Research Network (FCRN) (Coursolle et al., 2006), for example, would have substantially improved the network coverage of environmental space in the northwest. Furthermore, many of the Canadian and newer U.S. towers are disturbed (e.g., harvested, grazed, recently burned, managed, etc.) sites. These EC flux sites also include disturbance chronosequence (Amiro et al., 2010) and afforested chronosequence (Peichl et al., 2010) sites, representing disturbance histories and successional stages – important aspects that were not considered in previous analysis.

In this study, we used the EC flux data from the FLUXNET synthesis dataset (also known as the LaThuile database; http://www.fluxdata.org) for the 68 AmeriFlux sites and the 26 Fluxnet-Canada sites that were available from 2000 to 2007. The LaThuile database is based on a consistent data format, making it easier to manipulate and compare data from different instruments and among regions. This database standardizes and gap-fills the raw 30-min data records of carbon dioxide, water vapor, and energy fluxes submitted by members of regional networks from around the world.

2.2. MODIS data streams

The following data streams from the Moderate Resolution Imaging Spectroradiometer (MODIS) were used in this study: enhanced vegetation index (EVI) (Huete et al., 2002), land surface temperature (LST) (Wan et al., 2002), and surface reflectance (Schaaf et al., 2002). These data products are all at 1-km spatial resolution. The LST product is available at 8-day time interval, while EVI and surface reflectance are at 16-day time intervals. The surface reflectance product provides 1-km reflectance data adjusted using the bidirectional reflectance distribution function (BRDF) as if they were acquired from a nadir view, and represents the best characterization of surface reflectance over a 16-day period (Schaaf et al., 2002).

We used MODIS data products to develop the predictive flux models. For each EC site, we obtained the MODIS ASCII subsets for the period 2000–2007 from the Oak Ridge National Laboratory's Distributed Active Archive Center (ORNL DAAC). For each EC site, the ASCII subsets consist of 7 km × 7 km cutouts surrounding the tower. For each product, the quality assurance flag was used to determine the quality of each pixel for each 8-day or 16-day interval, and each value with poor quality was replaced with the nearest values with good quality using a linear interpolation approach. For each EC flux site, we extracted the average values of the pixels within the 3 km × 3 km area surrounding the tower for each variable. Although the tower footprint is typically much smaller than 9 km^2, we used the 3 km × 3 km area surrounding the tower rather than the single pixel in which the tower is located. The reason is threefold: first, the tower is often not located right in the middle of the 1 km pixel; second, the footprint of the tower is typically not a circle area surrounding the tower and is instead an upwind elliptical source area; third, the MODIS imagery has geolocation error.

For the continental-scale prediction of carbon fluxes, we obtained MODIS data products (EVI, LST, and surface reflectance) for the U.S. and Canada over the period 2000–2012. For each product and each 8-day or 16-day interval, the individual tiles were mosaicked to generate continental-scale maps. Similarly, for each product, the quality assurance flag was used to determine the quality of each pixel for each interval, and values with poor quality were replaced by the nearest values with good quality using a linear interpolation approach. For both MODIS ASCII subsets and continental-scale surface reflectance data, we calculated the normalized difference water index (NDWI) (Gao, 1996) from near-infrared and shortwave infrared bands. NDWI was shown to be strongly correlated with leaf water content (Jackson et al., 2004) and shallow soil moisture (Fensholt and Sandholt, 2003).

The MODIS land cover map (Friedl et al., 2010) with the University of Maryland classification scheme was used to specify the vegetation type of each pixel for the continental-scale prediction. The vegetation types were regrouped into the following seven broad vegetation types: evergreen forests, deciduous forests, mixed forests, shrublands, savannas, grasslands, and croplands (Fig. 1). Specifically, evergreen needleleaf forests and evergreen broadleaf forests were grouped into evergreen forests, deciduous broadleaf forests and deciduous needleleaf forests into deciduous forests, open shrublands and closed shrublands into shrublands, and woody savannas and savannas into savannas. We used the broad vegetation types rather than a more detailed classification scheme because the number of towers was limited for some vegetation types such as open shrublands and open savannas.

2.3. Climate data

We used photosynthetically active radiation (PAR) data from the North American Regional Reanalysis (NARR) dataset developed by the National Centers for Environmental Prediction (NECP) (Mesinger et al., 2006). The NCEP NARR is based on the NCEP Global Reanalysis, and has been improved for the North American domain. The improvements in the model/assimilation have led to substantial improvements in the accuracy of the NCEP NARR data compared to the NCEP-DEO Global Analysis 2 (Mesinger et al., 2006). The spatial resolution of the NARR dataset is approximately 0.3° (or

~30 km). We used PAR data from NARR from 2000 to 2012, and resampled the data to 1 km resolution to match the resolution of other driving data.

Despite the improvement of the NARR dataset, the PAR data exhibited systematic positive biases compared to the measured PAR data from the EC sites across the continent (Supplementary Fig. S1). We used the tower observations to calibrate the NARR PAR. It should be noted that the PAR (photoelectric) sensors at the EC flux sites gradually degrade over time and typically exhibit a drift of <2% per year (Schmidt et al., 2012) although high values (>10% per year) have been reported and thus annual calibration is needed (Fielder and Comeau, 2000). During the past 6 years, however, the AmeriFlux QA/QC reference PAR sensors have been sent to site for calibration, and the network has also encouraged annual calibrations by the manufacturer. As part of the AmeriFlux QA/QC effort, the lab-calibrated roving system PAR was compared with the PAR observations from 84 sites, and the comparisons showed that the relative instrument error (RIE) was small ($-3 \pm 14\%$), although the deviation around the mean was relatively large (Schmidt et al., 2012). The relative bias of NARR PAR compared to tower PAR is often much higher than 3% (Supplementary Fig. S1), and therefore calibrating the NARR PAR using tower observations could reduce the biases in the NARR PAR. We developed a linear regression model between the NARR PAR (PAR_{NARR}) and measured tower PAR (PAR_{tower}) ($PAR_{tower} = 0.70 \times PAR_{NARR} + 1.05$; $R^2 = 0.70$; the units of PAR are MJ m^{-2} d^{-1}), and then used the linear regression model to calibrate PAR values for all pixels across the continent. The calibrated PAR data were used for the prediction of carbon fluxes at the continental scale.

2.4. Spatial ecological data

Aboveground biomass data were used for our prediction of carbon fluxes. Site-level biomass data were obtained from the site descriptions and/or biological templates. Spatially explicit data on aboveground biomass has recently become available for North America (Zhang and Kondragunta, 2006; Blackard et al., 2008). Zhang and Kondragunta (2006) developed a continental-scale forest biomass (foliage biomass, branch biomass, and total aboveground biomass) at a spatial resolution of 1 km using foliage-based generalized allometric models and MODIS data. In addition, Blackard et al. (2008) developed a 1 km aboveground forest biomass dataset from ground measured inventory plots, remotely sensed data, climate data, and other ancillary variables for the conterminous U.S., Alaska, and Puerto Rico. For the continent, we combined these two aboveground biomass datasets. For the U.S., we used the 250 m-resolution aboveground biomass dataset (Blackard et al., 2008); for Canada, we used the continental-scale map derived from MODIS and allometric equations (Zhang and Kondragunta, 2006).

We also used the North American Forest Stand Age database derived from forest inventory, large fire polygons, and remotely sensed data (Pan et al., 2011b). This database provides stand age information for each 1 km forested grid cell across North America, and has been used in a continental-scale inversion study (Deng et al., 2013). We used the spatially explicit stand age information to improve the accuracy of flux estimates and to account for the effects of stand age and disturbance on forest carbon dynamics. The stand age of the forested EC flux sites used in this study generally captured the frequency distribution of stand age across the continent based on the continental-scale stand age map (Supplementary Fig. S2). However, the EC flux sites over-represented the frequency distribution for 0–15 years of age and under-represented the distribution for approximately 40–50, 70–90, 110–140, and 160–180 years of age (Supplementary Fig. S2).

A proxy of canopy nitrogen concentrations (%N) was used to account for the continuous variation in plant N status as a driver of carbon cycle processes at regional to continental scales. MODIS albedo and channel 2 near-infrared (NIR) reflectance data have been shown to be equally correlated with both leaf N concentrations (% by mass) and maximum photosynthetic rates over large areas (Ollinger et al., 2008). Admittedly, the relationship between albedo and canopy %N is not well established (Knyazikhin et al., 2013; Townsend et al., 2013). Despite its limitations, the tight relationship has been applied to parameterize Farquhar's photosynthesis model for the estimation of GPP (Ryu et al., 2011). We obtained a canopy %N database for 13 sites in Oregon. Canopy %N was measured for a total of 95 plots at these sites in 2000 and 2001. We extracted NIR reflectance integrated over the peak of the growing season from MODIS for each plot, and calculated the mean and standard deviation of canopy %N and NIR for each site. Canopy %N was significantly correlated with NIR across these sites (Supplementary Fig. S3), showing that NIR explained 30% of the variance in canopy %N in Oregon. In this study, we used the NIR integrated over the peak of the growing season to approximate canopy %N following Ollinger et al. (2008).

2.5. Data-driven approach

A data-driven approach (Xiao et al., 2008) was used to upscale fluxes from towers to the continental scale. This approach is essentially an ensemble of regression models, and generates rule-based predictive models. Each predictive model consists of a number of rule-based sub-models. Each sub-model is associated with a set of rules, each of which is a set of conditions associated with a multivariate linear submodel. The rules can overlap with one another. Altogether, these models can account for the nonlinear relationships between carbon fluxes and the explanatory variables. This method also allows both continuous and discrete variables. The predictive accuracy of a rule-based model can be improved by its combination with an instance-based/nearest-neighbor model predicting the target value of a new case using the average predicted values of the *n* most similar cases (RuleQuest, 2008). Our data-driven approach can generate an ensemble of rule-based models, and the average values from all the models are used to provide the final prediction. This approach has been described in detail in our previous publications (Xiao et al., 2008, 2010).

We developed a predictive model for each carbon flux at the site level using the EC flux data, MODIS data streams, and measured meteorological data. The explanatory variables included land cover type, EVI, LST, NDWI, PAR, canopy %N estimates, stand age, and aboveground biomass. These variables can account for the meteorological and ecological factors influencing GPP, ER, and NEP, and can thus be used to develop predictive models for these carbon fluxes (Xiao et al., 2008, 2010). Besides carbon fluxes, we also estimated evapotranspiration (ET) in order to assess the responses of carbon fluxes to drought.

Cross-validation was used to provide an estimate of the predictive accuracy of our predictive models. We used *k*-fold cross-validation, in which the cases are divided into *k* blocks of roughly the same size and target value distribution. For each block, a predictive model is developed based on the cases in the remaining blocks, while the cases in the hold-out block is then used to test the model performance (RuleQuest, 2008). We then used the predictive models to estimate fluxes for each 1 km × 1 km grid cell across North America for each 8-day interval over the period 2000–2012. The 8-day interval was chosen to match the compositing period of MODIS data products. Compositing is typically used for MODIS data products to minimize the effects of cloud contamination. We then

Table 1
Cross-validation of the predictive models for carbon and water fluxes for both forest and non-forests. For RMSE, the units are $g\,C\,m^{-2}\,d^{-1}$ for carbon fluxes and $mm\,d^{-1}$ for ET.

Flux	Vegetation type	Regression equation	*p*-value	R^2	RMSE
GPP	Forests	$y = 0.92x + 0.30$	<0.001	0.91	1.01
	Non-forests	$y = 0.89x + 0.28$	<0.001	0.89	1.37
ER	Forests	$y = 0.84x + 0.44$	<0.001	0.82	1.02
	Non-forests	$y = 0.88x + 0.23$	<0.001	0.87	0.80
NEP	Forests	$y = 0.84x + 0.10$	<0.001	0.83	0.72
	Non-forests	$y = 0.80x + 0.08$	<0.001	0.80	1.08
ET	Forests	$y = 0.92x + 0.10$	<0.001	0.91	0.32
	Non-forests	$y = 0.89x + 0.15$	<0.001	0.88	0.44

used the 13-year gridded flux dataset to examine the magnitude, distribution, and interannual variability of carbon fluxes over North America.

3. Results and discussion

3.1. Evaluation of our predictive models

The cross-validation results showed that our data-driven predictive models estimated carbon and water fluxes fairly well at the site level (Fig. 2; Table 1). The R^2 values ranged from 0.80 to 0.91 and the root mean squared error (RMSE) values ranged from 0.72 to 1.37 $g\,C\,m^{-2}\,d^{-1}$ across carbon fluxes. For ET, the R^2 values ranged from 0.88 to 0.91, and the RMSE values ranged from 0.32 to 0.44 $mm\,d^{-1}$. GPP and ET exhibited higher R^2 values than ER and NEP, suggesting that GPP and ET were slightly better estimated than ER and NEP. This is mainly because the explanatory variables used in our approach could better account for the controlling factors of GPP and ET than those of ER and NEP. Although the explanatory variables could partly account for air temperature, canopy water content, aboveground biomass, and stand age, soil substrate availability was not explicitly considered. Substrate availability is an important controlling factor of ER and NEP (Davidson et al., 2006).

For forest sites, the addition of stand age and aboveground biomass into the predictive models reduced the mean absolute error (MAE) (Xiao et al., 2010) by 16.9% for GPP, 14.8% for NEP, and 13.2% for ER, while the addition of the proxy for canopy %N (NIR integrated over the peak of the growing season) to the models with stand age and aboveground biomass already included reduced the MAE by an additional 3.3% for GPP, 4.2% for NEP, and 1.7% for ER. For non-forest sites, the addition of the proxy for canopy %N into the predictive models reduced the MAE by 16.3% for GPP, 13.5% for NEP, and 16.4% for ER.

For GPP, NEP, and ET, forests exhibited lower RMSE and slightly higher R^2 values than non-forests, showing that our approach had slightly higher accuracy for forests than for non-forests for these fluxes. For ER, forests had higher RMSE and slightly lower R^2 values than non-forests for ER, showing that our approach had slightly lower accuracy for forest ER than non-forest ER. The remotely sensed data streams that we used could better capture the properties of litter layers and soils for non-forests than for forests. Litter significantly affects the spectral signature of grasslands, and a small increase in litter fractional cover can have a disproportionately large effect on canopy reflectance (Asner, 1998). Moreover, the MODIS-derived LST was closer to soil surface temperature for non-forests than for forests, while soil respiration has been widely simulated as a function of soil temperature (Lloyd and Taylor, 1994). Our data-driven approach could thus better capture ER for non-forests than for forests.

3.2. Magnitude and spatial distribution of annual carbon fluxes

The mean annual carbon fluxes over the period 2001–2012 varied substantially over space (Fig. 3). GPP and ER generally exhibited similar spatial patterns, although GPP was systematically higher than ER in most regions. The southeastern U.S. and the northern Pacific Coast of U.S. and Canada exhibited the highest annual GPP ($\sim$1500–2000 $g\,C\,m^{-2}\,yr^{-1}$) and ER ($\sim$1000–1500 $g\,C\,m^{-2}\,yr^{-1}$). These regions had the highest GPP because of favorable temperature and precipitation (soil moisture) conditions. Some regions in the Pacific Coast assimilated carbon even in the winter because of the dominance of evergreen forests and mild temperatures in the regions (Waring and Franklin, 1979; Anthoni et al., 2002). The Midwest, the Great Plains, the Rocky Mountains, and the forest regions of Canada had intermediate GPP ($\sim$800–1200 $g\,C\,m^{-2}\,yr^{-1}$) and ER ($\sim$600–800 $g\,C\,m^{-2}\,yr^{-1}$). Many areas in the western U.S., northern Canada, and Alaska exhibited low GPP and ER (<500 $g\,C\,m^{-2}\,yr^{-1}$) because of sparse vegetation, precipitation deficits, or lower temperatures and shorter growing seasons.

NEP generally exhibited similar spatial patterns to GPP and ER. Overall, the eastern U.S. and the Pacific Coast exhibited the highest annual NEP ($\sim$300–600 $g\,C\,m^{-2}\,yr^{-1}$); the forested region of Canada and the Rocky Mountains in the U.S. exhibited intermediate NEP ($\sim$100–200 $g\,C\,m^{-2}\,yr^{-1}$). A part of the Southwest provided minor carbon sources, while the small region in northeastern Arizona and southeastern Utah exhibited annual NEE of >200 $g\,C\,m^{-2}\,yr^{-1}$. This region was affected by moderate to severe drought in 2000–2003 and 2005, which likely resulted in a net carbon loss. In addition, our predictive model utilized LST to account for ER, and the explanatory variables could not account for the sizes of soil carbon pools and litter. The relatively high temperatures in this region in the summer and the inability of our predictive model to account for soil carbon pools and litter may lead to reduced net carbon uptake or net carbon loss. Many areas in the western U.S., northern Canada, and Alaska had low NEP and were nearly carbon neutral. The spatial patterns of annual carbon fluxes were largely determined by climate, vegetation type, and forest stand age (disturbance and management history) (Xiao and Moody, 2004; Amiro et al., 2010; Peichl et al., 2010).

Unlike our previous upscaling studies for the conterminous U.S. (Xiao et al., 2008, 2010, 2011a), this study used the recently available ecological data: aboveground biomass (Zhang and Kondragunta, 2006; Blackard et al., 2008), stand age (Pan et al., 2011b), and a proxy for canopy %N (Ollinger et al., 2008). Our new GPP and NEP estimates were slightly lower than our previous estimates (Supplementary Fig. S4), particularly in the southeastern U.S., mainly because of the use of the new ecological data. Our new flux estimates are likely more accurate than our previous estimates. For example, our previous annual NEP estimates (Xiao et al., 2011a) were higher than 600 $g\,C\,m^{-2}\,yr^{-1}$ in many areas in the southeast and were slightly higher than expected.

3.3. Annual GPP, ER, and NEP of the U.S. and Canada

The mean annual GPP, ER, and NEP of the U.S. over the period 2001–2012 were 6.84, 5.31, and 1.10 $Pg\,C\,yr^{-1}$, respectively. The mean annual nationwide fluxes varied by vegetation type (Fig. 4). For the U.S., croplands had the highest total annual GPP, ER, and NEP. Similarly, croplands had the highest mean annual ET. It should be noted that C_4 and C_3 crops were not discriminated and tillage management (e.g., no tillage, low tillage, or full tillage) was not explicitly considered in this study, which might limit the accuracy of cropland flux estimates. Although irrigation/non-irrigation was not explicitly incorporated, EVI and NDWI could account for the effects of drought and soil moisture stress. Altogether, U.S.

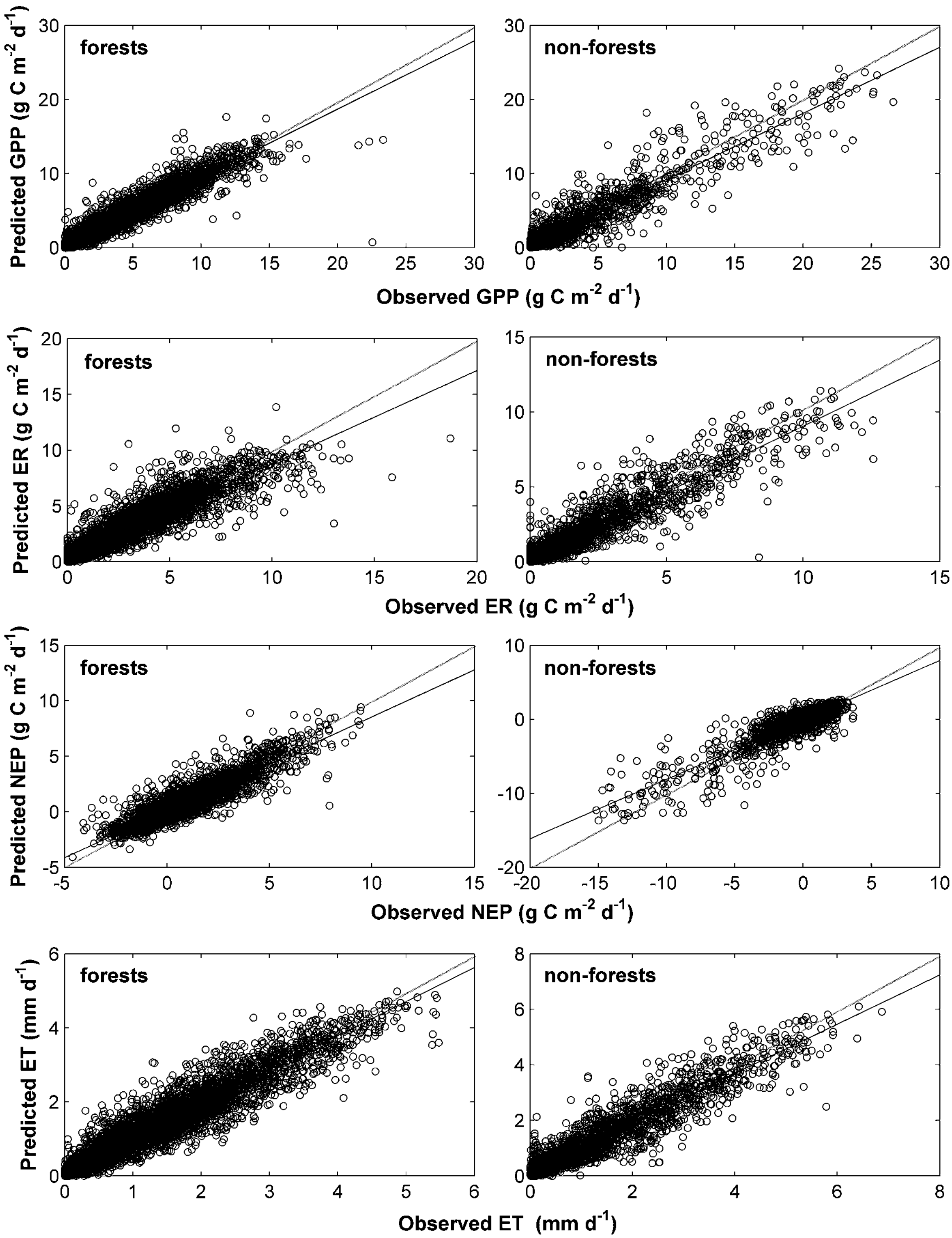

Fig. 2. Cross-validation of the predictive models for carbon and water fluxes for North America: GPP for forests (a) and non-forests (b); ER for forests (c) and non-forests (d); NEP for forests (e) and non-forests (f); and ET for forests (g) and non-forests (h).

forests accounted for 35.0%, 32.5%, and 42.7% of the total GPP, ER, and NEP, respectively, which were comparable to those of croplands (36.5%, 38.7%, and 40.0%, respectively). The ET of U.S. forests (812.9 km^3, or 402.2 mm yr^{-1}) was lower than that of croplands (1263.7 km^3, or 557.0 mm yr^{-1}). Compared with our previous studies (Xiao et al., 2008, 2010, 2011a), here we used recently available, spatially explicit data layers on stand age (Pan et al., 2011b), aboveground biomass (Zhang and Kondragunta, 2006), and canopy nitrogen estimates (Ollinger et al., 2008). For the period 2001–2006, our new estimate of the mean annual GPP of the conterminous U.S. was 6.89 Pg C yr^{-1}, which was 2.4% lower than our previous estimate (Xiao et al., 2010); our new NEP estimates for natural ecosystems and croplands of the conterminous U.S. were 0.54 and 0.44 Pg C yr^{-1}, which were 14.3% and 24.1% higher than our previous estimates (0.63 and 0.58 Pg C yr^{-1}) (Xiao et al., 2011a), respectively.

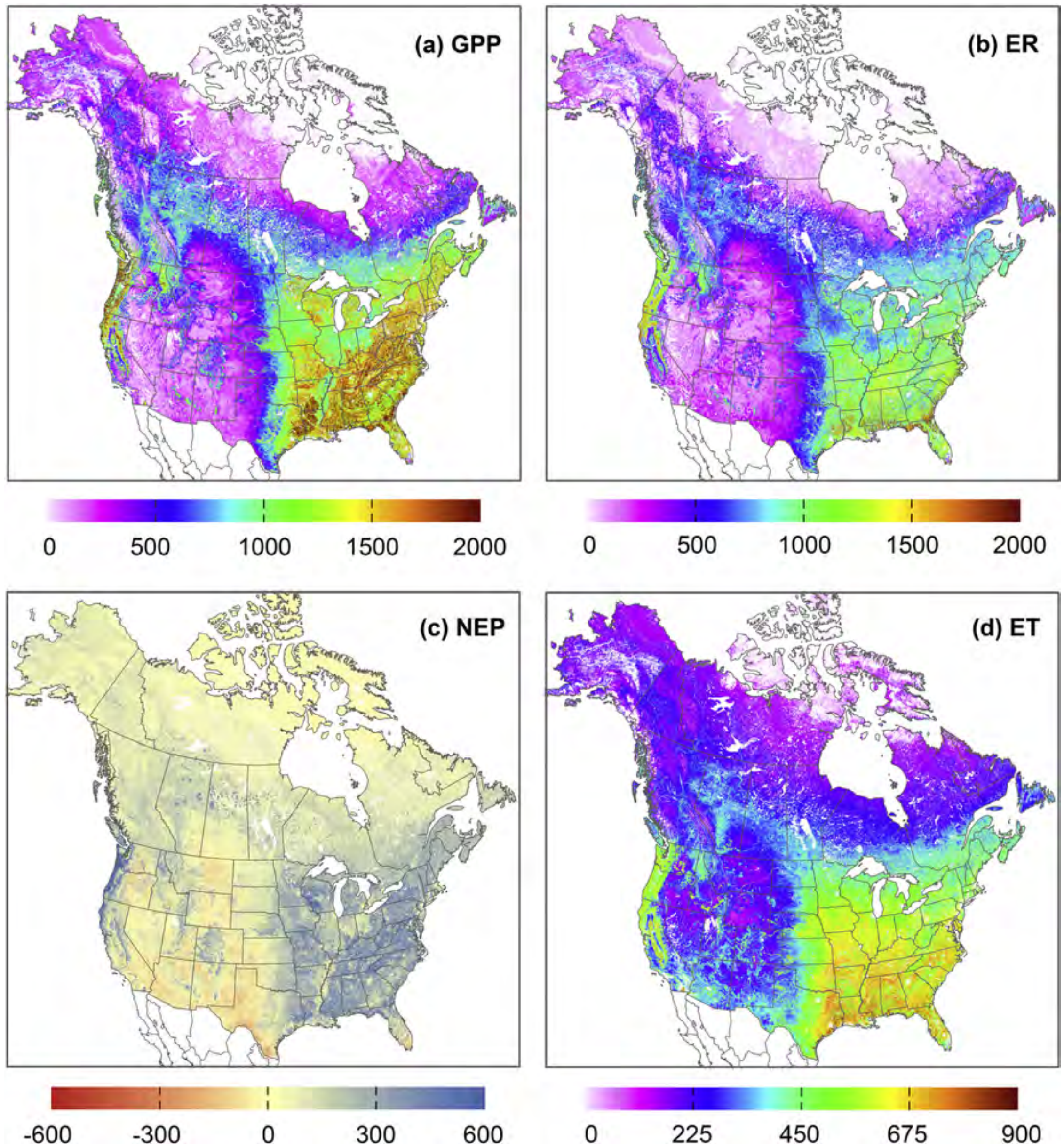

Fig. 3. Mean annual carbon and water fluxes over North America for the period 2001–2012: (a) GPP); (b) ER; (c) NEP; and (d) ET. The units for carbon fluxes are $g\,C\,m^{-2}\,yr^{-1}$, and the units for ET are $mm\,yr^{-1}$.

The mean nationwide annual NEP of natural ecosystems over the period 2001–2012 was $0.53\,Pg\,C\,yr^{-1}$ for the U.S. and $0.49\,Pg\,C\,yr^{-1}$ for the conterminous U.S. Biomass burning emissions were not included in our estimate. If fire emissions ($0.06\,Pg\,C\,yr^{-1}$) (Wiedinmyer, 2007) were deducted from our estimate, then the size of the carbon sink for the conterminous U.S. was $0.43\,Pg\,C\,yr^{-1}$, which was 24.6% lower than our previous estimate ($0.57\,Pg\,C\,yr^{-1}$) (Xiao et al., 2011a). Our estimate was similar to the estimate ($0.49\,Pg\,C\,yr^{-1}$) of the first State of the Carbon Cycle Report (SOCCR, 2007) and is also within the range ($0.30–0.58\,g\,C\,yr^{-1}$) of an earlier estimate (Pacala et al., 2001). Our approach makes use of continuous flux observations from EC flux towers that represent direct samples of net CO_2 exchange from sites encompassing a variety of North American biomes and climate types. These data were not utilized in most previous U.S. carbon budget studies (Houghton et al., 1999; Schimel et al., 2000; Pacala et al., 2001; SOCCR, 2007).

The mean annual GPP, ER, and NEP of Canada over the 12-year period were 3.91, 3.26, and $0.60\,Pg\,C\,yr^{-1}$, respectively. Our GPP estimate for Canada's landmass is 45.6% higher than a recent estimate ($2.68\,Pg\,C\,yr^{-1}$) based on an ecosystem model (Gonsamo et al., 2013). Evergreen forests had the highest contribution to Canada's annual GPP, ER, and NEP; mixed forests, shrublands, and croplands had intermediate contributions; deciduous forests, savannas, and grasslands had the lowest values (Fig. 4). Evergreen forest lands and savannas had the largest fraction of total annual ET; mixed forests and croplands had intermediate contributions to total ET; deciduous forests, shrublands, and grasslands the lowest contribution to total Canadian ET (Fig. 4).

Our mean annual NEP of natural ecosystems for Canada over the period 2001–2012 was $0.55\,Pg\,C\,yr^{-1}$, which was higher than previous estimates of Canada's terrestrial carbon sink. Previous estimates for net biome productivity (NBP) for Canada's forests ranged from -0.10 to $0.25\,Pg\,C\,yr^{-1}$ (Kurz and Apps, 1999; Chen et al., 2000, 2003). A recent forest inventory study estimated the carbon sink of Canada's forests to be $0.01\,Pg\,C\,yr^{-1}$ for the period 2000–2007 (Pan et al., 2011b). It should be noted that our estimates did not include fire emissions and the mortality induced by mountain pine beetle outbreaks in western Canada and droughts in

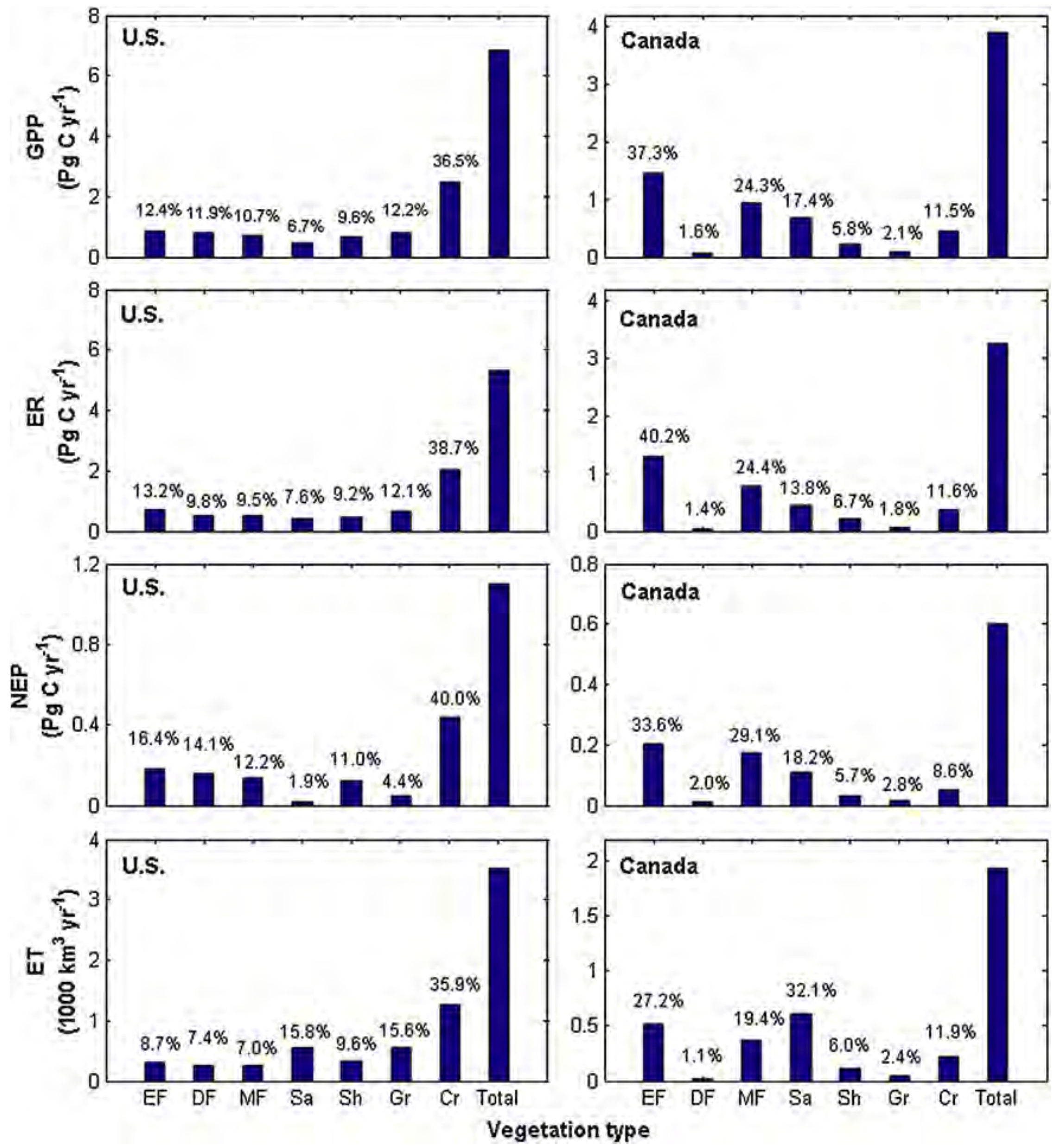

Fig. 4. Total annual carbon and water fluxes averaged over the period 2001–2012 for the U.S. and Canada at the national scale and for each broad vegetation type. The broad vegetation types are: evergreen forests (EF), deciduous forests (DF), mixed forests (MF), savannas (Sa), grasslands (Gr), and croplands (Cr). The percentages stand for the proportions that each broad vegetation type accounts for the nationwide fluxes.

central Canada. Scaling the area burned for the 2001–2012 period for Canada (2×10^4 km^2 yr^{-1}; CIFFC, 2014) with emission estimates (Amiro et al., 2009) gives a fire combustion emission of about 0.024 Pg C yr^{-1}. In British Columbia alone, the outbreaks of mountain pine beetle led to the release of 0.27 Pg C during 2000–2020 (Kurz et al., 2008). With fire emissions and the effects of insect outbreaks deducted, our estimate of Canada's carbon sink was still higher than previous estimates.

We compared our sink estimates against results from a nested atmospheric inversion model (Deng and Chen, 2011). Deng and Chen (2011) used an atmospheric CO_2 inversion approach to quantify carbon sinks and sources at regional scales by dividing North America into 28 regions. There was a fairly good linear relationship between our net flux estimates and the inversion results (Fig. 5). This enhanced our confidence in our continental-scale flux estimates given the fact that our method was a bottom-up approach and the inversion results were based on a top-down approach. Nevertheless, our sink estimates were much higher than the inversion results. Our estimates overestimated the magnitude of carbon sinks for some regions compared to the inversion likely because the effects of fire emission and bark beetle disturbances were not fully considered and our approach cannot capture the direct emissions from fire disturbance. In addition, our approach cannot account for heterotrophic respiration well because of lack of spatially explicit information on the sizes and changes in soil organic carbon and litterfall. Our estimates therefore are essentially NEP, not net biome productivity (NBP) as estimated by the inversion.

3.4. Interannual variability in carbon fluxes of the U.S. and Canada

The carbon fluxes exhibited year-to-year variations during the period from 2001 to 2012 (Fig. 6). For the U.S., GPP exhibited relatively large interannual variability with the highest GPP in

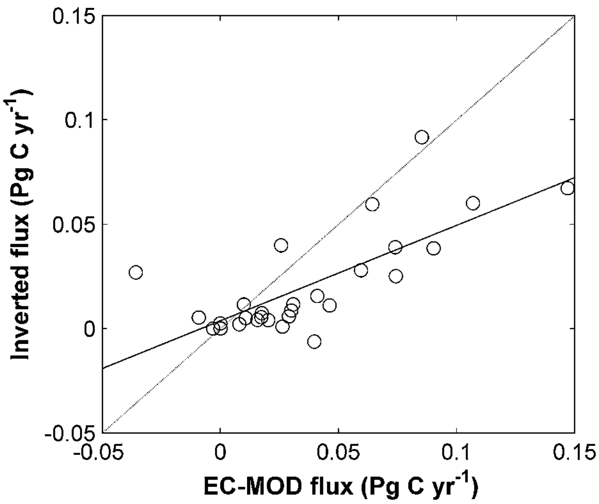

Fig. 5. Comparison of our annual NEP estimate (EC-MOD) against the inverted flux from a nested atmospheric inversion model.
Deng et al. (2011).

2007 (7.29 Pg C yr^{-1}) and the lowest GPP in 2011 (6.51 Pg C yr^{-1}), and the GPP of 2007 was 12.0% higher than that of 2011. The annual GPP of 2002, 2006, 2009, and 2012 were also relatively low. The annual ER exhibited slightly smaller variability with the highest ER in 2007 (5.60 Pg C yr^{-1}) and the lowest flux in 2002 (5.10 Pg C yr^{-1}), and the ER of 2007 was 9.8% higher than that of 2011. NEP also exhibited relatively larger interannual variability than either GPP or ER with the highest NEP in 2005 (1.25 Pg C yr^{-1}) and the lowest NEP in 2009 (0.90 Pg C yr^{-1}); NEP of 2005 was 38.9% higher than that of 2009. Three years (2001, 2007, and 2010) had relatively high annual NEP, while other years (2002, 2006, 2011, and 2012) had relatively low NEP.

For Canada, GPP, NEP, and ET exhibited relatively larger interannual variability than ER (Fig. 6). The years of 2001, 2005, 2006, 2010, and 2012 had high GPP and ER; 2003, 2004, 2007, 2008, 2011 had intermediate fluxes; 2002 and 2009 had low GPP and ER. Similar to that of the U.S., the NEP of Canada also exhibited relatively large interannual variability with the highest NEP in 2005 (0.67 Pg C yr^{-1}) and the lower NEP in 2009 (0.53 Pg C yr^{-1}). NEP in 2005 was 26.4% higher than that in 2009. Both 2004 and 2007 had slightly lower NEP (0.65 Pg C yr^{-1}) than 2005. The year of 2002 also had low NEP (0.54 Pg C yr^{-1}).

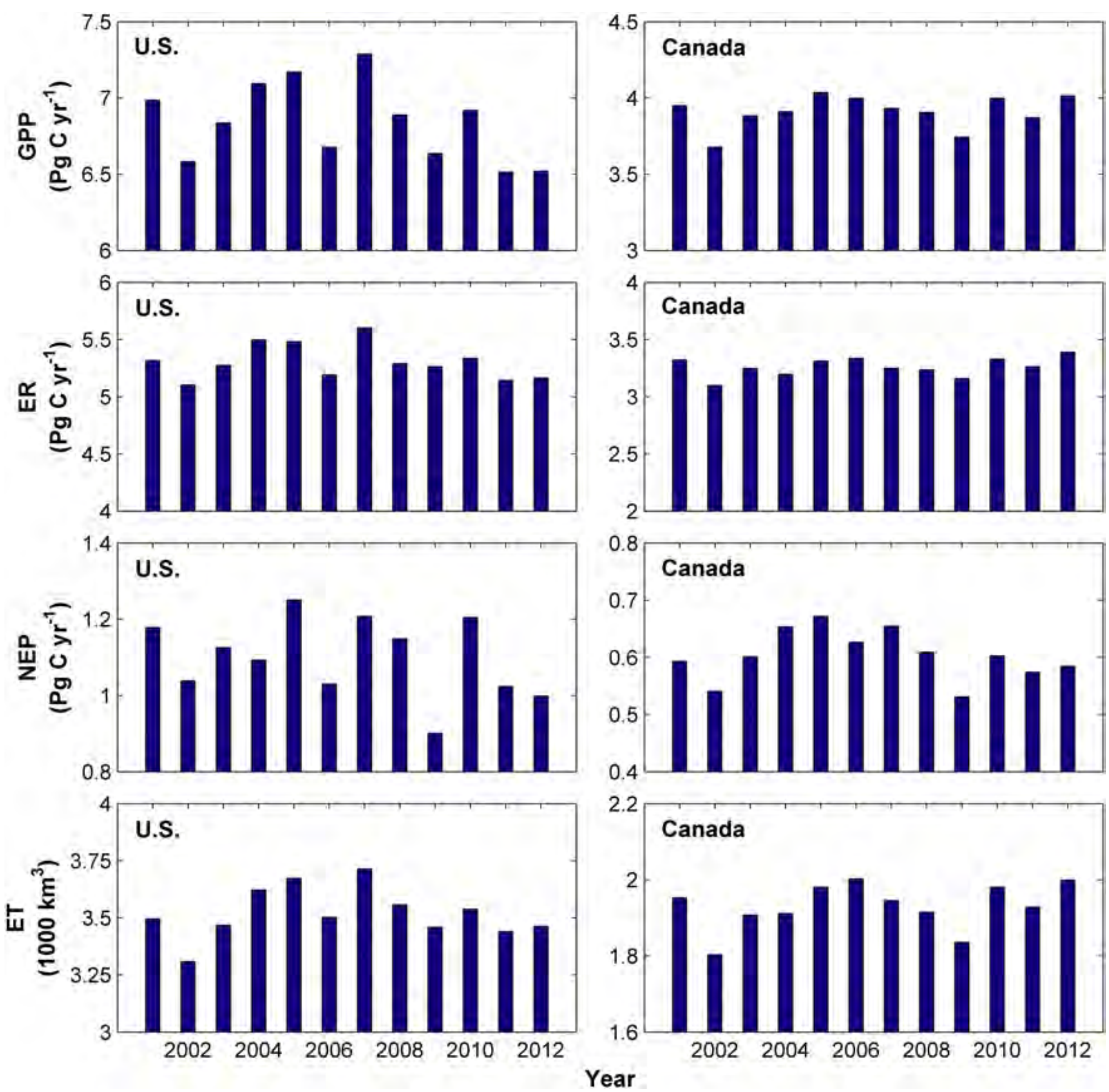

Fig. 6. Annual carbon and water fluxes for the U.S. and Canada for each year over the period 2001–2012.

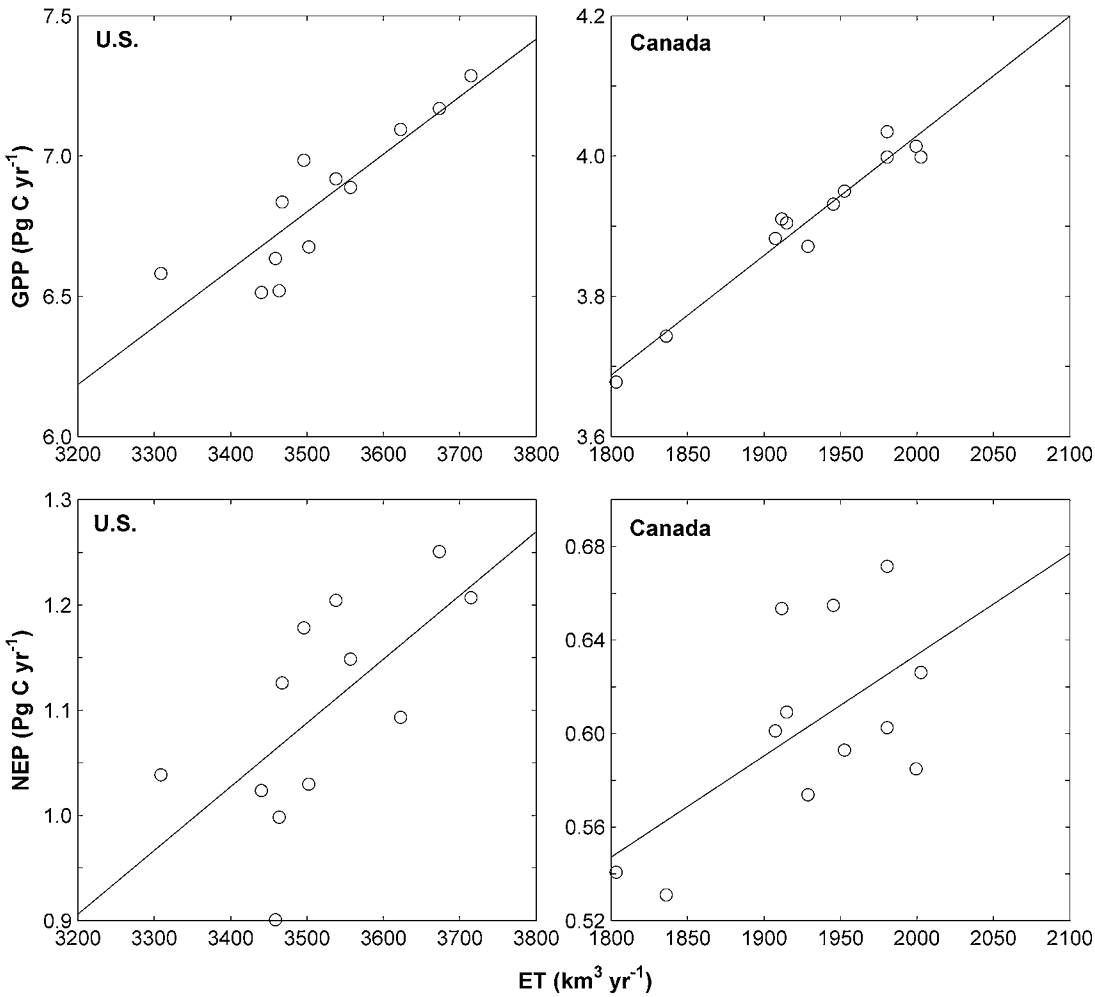

Fig. 7. Relationships of annual GPP and NEP with annual ET for the U.S. and Canada over the period 2001–2012.

The main sources of the interannual variability in the carbon fluxes over North America included drought and disturbance. The annual ET of the U.S. exhibited relatively large interannual variability with the highest ET in 2007 (3714.4 $km^3 yr^{-1}$) and the lowest value in 2002 (3308.7 $km^3 yr^{-1}$), and the ET of 2007 was 12.3% higher than that of 2002. The years of 2004 and 2005 also had relatively high ET, and others years had intermediate or low ET. The annual ET ($km^3 yr^{-1}$) was strongly correlated with annual GPP ($Pg C yr^{-1}$) for the U.S. ($ET = 0.002 \times GPP - 0.39$, $R^2 = 0.76$, $p < 0.001$) and Canada ($ET = 0.002 \times GPP + 0.62$, $R^2 = 0.95$, $p < 0.001$) (Fig. 7). There were moderate relationships between annual ET ($km^3 yr^{-1}$) and annual NEP ($Pg C yr^{-1}$) for both the U.S. ($ET = 0.0006 \times NEP - 1.03$, $R^2 = 0.42$, $p < 0.05$) and Canada ($ET = 0.0004 \times NEP - 0.23$, $R^2 = 0.38$, $p < 0.05$) (Fig. 7). These results demonstrated that the carbon and water cycles are closely coupled, and low ET associated with large water deficits can lead to significant declines in carbon fluxes.

We used the Palmer Drought Severity Index (PDSI) (Palmer, 1965) to delineate the extent and severity of drought. The global PDSI data with 0.5° spatial resolution (Zhao and Running, 2010) was used in this study. North America experienced frequent severe droughts during the study period. For example, drought affected 41.5%, 27.8%, and 19.2% of North America in 2002, 2006, and 2011, respectively (Fig. 8). In many areas affected by drought, annual ET exhibited negative anomalies. The negative anomalies in ET corresponded to negative anomalies in both GPP and ER. Annual GPP exhibited relatively larger reduction in drought years than annual ER did, leading to a reduction in annual NEP. This is consistent with recent findings based on modeling (Xiao et al., 2009) and EC flux data (Schwalm et al., 2010).

Large fires also led to declines in regional carbon fluxes (Figs. 9 and 10). Fig. 9 shows anomalies of annual carbon and water fluxes within large fire polygons. These fire polygons were obtained from the historical large fire database for Alaska from the Bureau of Land Management, Alaska Forest Service (http://afsmaps.blm.gov). According to the database, there were 160 large fires in Alaska in 2004, and altogether, these fires burned 2.7×10^4 km^2 of land. The information on the type of primary fuel is available for 70 of the fires: 37.1% of the 70 fires were tundra, brushes, and grass, and the remainder was black spruce. The carbon fluxes (GPP, ER, and NEP) exhibited negative anomalies within the fire polygons. However, the fires did not lead to large anomalies in ET. Similarly, annual carbon fluxes exhibited anomalies within fire polygons in Canada (Fig. 10). The fire polygons were obtained from the Canadian Large Fire Database (LFDB) from the Canadian Forest Service (Stocks et al., 2002). The decline in GPP was larger than that in ER, leading to a decline in NEP. The annual ET also exhibited negative anomalies within fire polygons. In 2005, fires burned 1.9×10^4 km^2 of land in Canada. The large fires in the U.S. and Canada led to declines in annual carbon fluxes. Our previous studies also showed that hurricanes can also reduce regional carbon uptake (Xiao et al., 2010, 2011a).

Our results showed that drought and disturbances had substantial impacts on carbon fluxes at regional to continental scales.

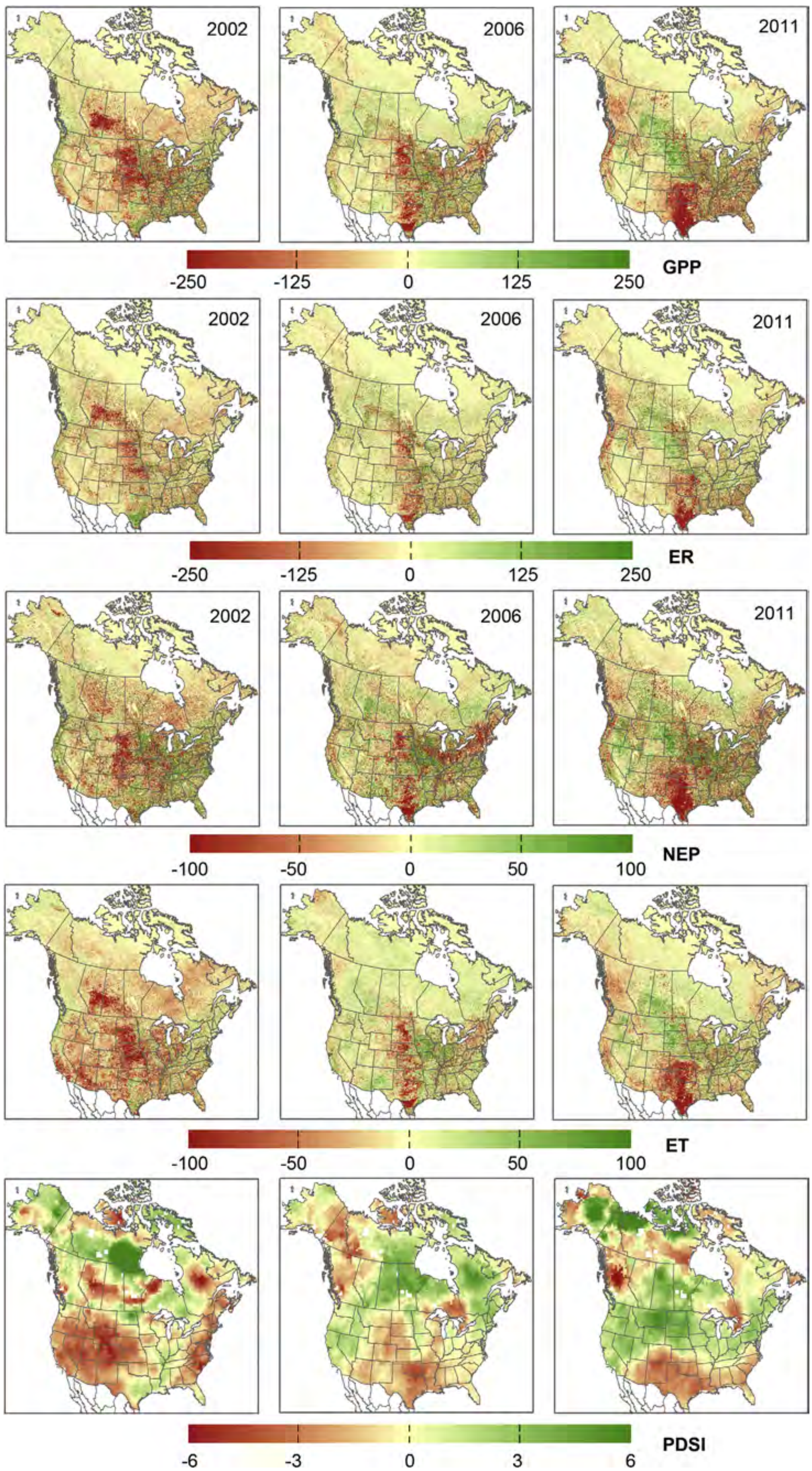

Fig. 8. Anomalies of annual carbon and water fluxes and annual PDSI for 2002, 2006, and 2011. The anomalies are relative to the means over the period 2001–2012. The units for carbon fluxes are $g\,C\,m^{-2}\,yr^{-1}$ and the units for ET are $mm\,yr^{-1}$.

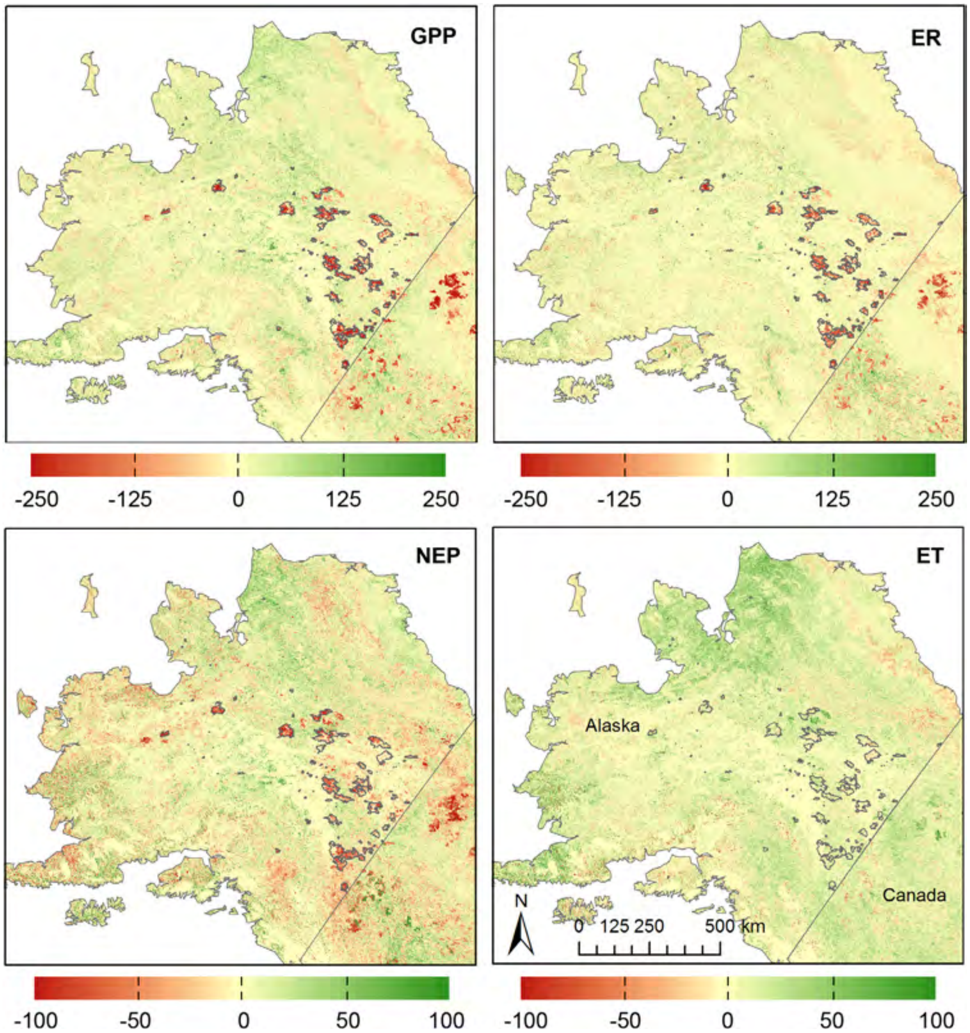

Fig. 9. Anomalies of carbon and water fluxes in Alaska in 2005. The anomalies are relative to the means over the period 2001–2012. The gray polygons are the large fire polygons. The units of carbon fluxes are g C m yr^{-1} and the units of ET are mm yr^{-1}.

Chronosequence and modeling studies have also showed disturbances such as fire, hurricanes, wind storms, and insect outbreaks substantially alter carbon fluxes in North America (Kurz et al., 2008; Amiro et al., 2010; Liu et al., 2011). Drought is projected to become more frequent and more severe in the mid-latitudes during the remainder of the 21st century under different climate change scenarios (IPCC, 2007). Extreme climate events and disturbances will likely have larger impacts on the terrestrial carbon cycle over North America.

3.5. Sources of uncertainty

Our flux estimates are associated with several sources of uncertainty. First, the spatial data that we used for the prediction of carbon fluxes at the continental scales have significant uncertainty. For example, the stand age (Pan et al., 2011a) and aboveground biomass (Zhang and Kondragunta, 2006; Blackard et al., 2008) data sets likely have substantial uncertainty. The main sources of uncertainty in the stand age map include older, inconsistent, and coarse resolution inventory data, incomplete data of unmanaged northern boreal forests, inaccurate determination of age at FIA sample plots, use of average ages for uneven-aged stands, and the algorithm for dating/mapping fire scar areas (Pan et al., 2011b). The remote sensing dating/mapping approach alone could introduce errors of ∼±7 yr (Chen et al., 2003). The U.S. forest biomass map had significant uncertainty, with the relative error ranging from 0.51 to 0.92 for different geographical regions (Blackard et al., 2008). Uncertainty in land cover classification (Friedl et al., 2010) is likely the most complex case because it affects the suite of parameters specified for an area and introduces errors into flux estimates. The overall accuracy of the MODIS land cover map was about 75% (Friedl et al., 2010), indicating that the biases in the land cover map could introduce significant uncertainty to the flux estimates.

Second, the EC flux data used to develop the predictive models also have uncertainty. For example, the EC observations contain significant uncertainty including systematic errors from insensitivity to high-frequency turbulence, random errors from inadequate sample size associated with averaging period, vertical and horizontal advection issues, and selection criteria for removing periods of inadequate mixing or low turbulence (Hollinger and Richardson, 2005; Loescher et al., 2006). Moreover, the gap-filling techniques used to fill EC data gaps can introduce uncertainty on the order of ±25 g C m^{-2} yr^{-1} (Moffat et al., 2007). Despite the larger number of EC sites, some geographical regions, vegetation types, and climate types are still under-represented. The under-representativeness of EC flux towers will presumably affect our flux estimates. In our analysis, carbon flux estimates will exhibit larger uncertainties in regions under-represented by towers.

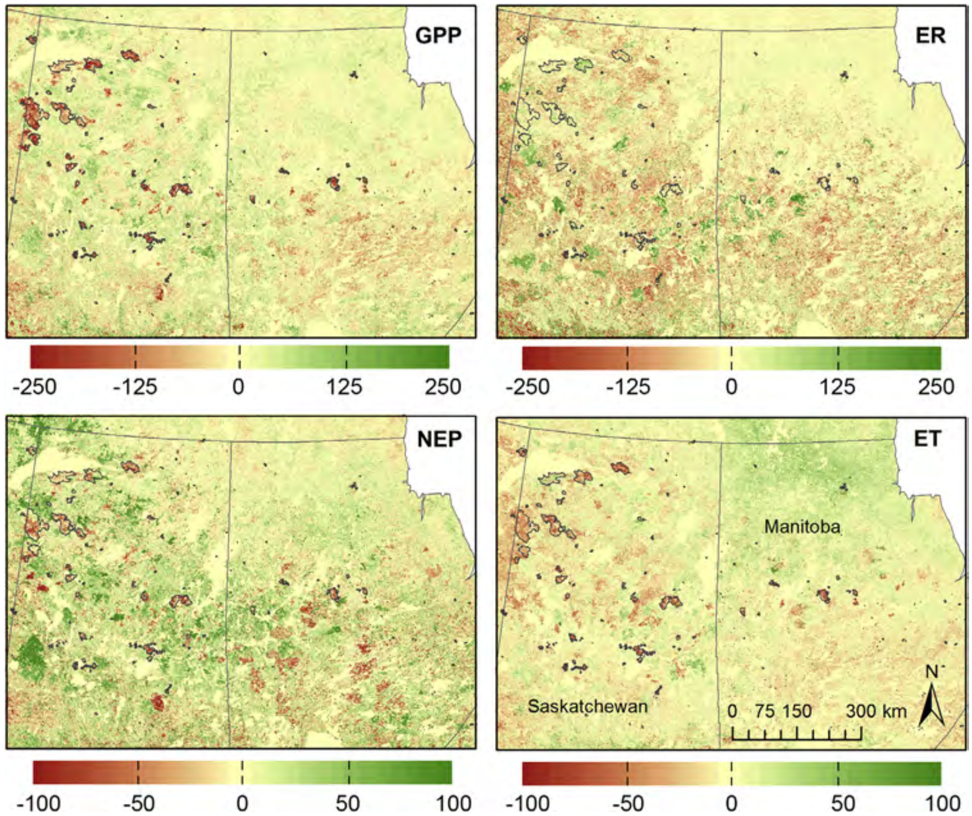

Fig. 10. Anomalies of carbon and water fluxes in Canada in 2005. The anomalies are relative to the means over the period 2001–2012. The gray polygons are the large fire polygons. The units of carbon fluxes are g C m yr^{-1} and the units of ET are mm yr^{-1}.

Third, our approach does not account for some controlling factors of carbon fluxes. For example, our approach cannot account for factors such as the magnitude and dynamics of soil organic carbon pools as well as disturbance type. Moreover, the spatial data layers including land cover and aboveground biomass were both static layers and constant were for 2001–2012. In reality, the land cover type may have changed over the study period due to forest management and land use activities, succession, or stand-replacing disturbances. Aboveground biomass pools could also have changed over the study period, especially for young and fast growing forest stands. Future efforts should incorporate dynamic land cover products, although the derivation of dynamic land cover and biomass data remains a challenge because of the substantial uncertainty in land cover classification and change detection.

Finally, we did not distinguish C_4 and C_3 crops in the Midwest because the lack of spatially explicit information on the type of photosynthesis pathway at the continental scale. The C_4 photosynthesis pathway has higher rate of leaf photosynthesis than plants with the C_3 pathway, but some studies showed that there was no consistent difference between the two groups (Snaydon, 1991). Moreover, we did not explicitly account for agricultural management practices.

The quantification of the uncertainty in our gridded flux estimates is beyond the scope of this study given the various sources and complex nature of the uncertainty. The assessment of full uncertainty remains a challenge in the realm of terrestrial ecosystem modeling. Current approaches are used to assess the uncertainty from different sources such as input data (Zhang et al., 2007; Xiao et al., 2011b), model parameters (Verbeeck et al., 2006; Xiao et al., 2014), and model structure (Wang et al., 2011; Huntzinger et al., 2012). We previously quantified the uncertainty in carbon fluxes resulting from the uncertainty in land cover maps (Xiao et al., 2011b) and model parameters (Xiao et al., 2014). New techniques are still needed to quantify the full uncertainty of flux estimates at regional to continental scales.

4. Conclusions

Our data-driven approach could estimate carbon fluxes fairly well and upscale flux observations from AmeriFlux and Fluxnet-Canada sites to the continental scale. Our gridded flux estimates provide independent, alternative estimates to recent North American ecosystem carbon exchange from March 2000 to December 2012 compared to conventional inventory approaches, ecosystem modeling, and atmospheric inversion. The mean annual GPP, ER, and NEP of the U.S. over the period 2001–2012 were 6.84, 5.31, and 1.10 Pg C yr^{-1}, respectively; the mean annual GPP, ER, and NEP of Canada over the 12-year period were 3.91, 3.26, and 0.60 Pg C yr^{-1}, respectively. Our estimate of the U.S. carbon sink is almost identical with that of the first SOCCR report. The carbon fluxes of North America exhibited relatively large interannual variability during the study period. The dry years of 2002, 2006, 2009, 2011, and 2012 had relatively low annual NEP, particularly for the U.S. The main sources of the interannual variability in the carbon fluxes over North America included drought and disturbance. These extreme events are expected to become more frequent and more severe during the remainder of the 21st century, and they will likely have lager impacts on the terrestrial carbon dynamics over North America.

Acknowledgements

This work was supported by the National Science Foundation through the MacroSystems Biology Program (award number 1065777) and the National Aeronautics and Space Administration

(NASA) through the Terrestrial Ecology program (award numbers NNX10AO03G, NNX11AB88G, and NNX12AK56G) and the Carbon Monitoring System (CMS) (award number NNX11AL32G). This work is part of the North American Carbon Program (NACP) research. We thank all AmeriFlux and Fluxnet-Canada PIs and their research personnel for making the flux observations available. The Fluxnet-Canada Research Network was funded by the Canadian Foundation for Climate and Atmospheric Sciences (CFCAS), the Natural Sciences and Engineering Research Council (NSERC) of Canada, BIOCAP Canada, Natural Resources Canada and Environment Canada. The financial support to the eddy covariance data harmonization of the LaThuile database was provided by CarboEuropeIP, FAO-GTOS-TCO, iLEAPS, Max Planck Institute for Biogeochemistry, National Science Foundation, University of Tuscia, Université Laval and Environment Canada and US Department of Energy and the database development and technical support from Berkeley Water Center, Lawrence Berkeley National Laboratory, Microsoft Research eScience, Oak Ridge National Laboratory, University of California – Berkeley, University of Virginia. We thank the two anonymous reviewers for their constructive comments on the manuscript.

Appendix A. Supplementary data

Supplementary data associated with this article can be found, in the online version, at http://dx.doi.org/10.1016/j.agrformet.2014.06.013.

References

Ainsworth, E.A., Long, S.P., 2005. What have we learned from 15 years of free-air CO_2 enrichment (FACE)? A meta-analytic review of the responses of photosynthesis, canopy. New Phytol. 165, 351–371.

Amiro, B.D., Barr, A.G., Barr, J.G., Black, T.A., Bracho, R., Brown, M., Chen, J., Clark, K.L., Davis, K.J., Desai, A.R., Dore, S., Engel, V., Fuentes, J.D., Goldstein, A.H., Goulden, M.L., Kolb, T.E., Lavigne, M.B., Law, B.E., Margolis, H.A., Martin, T., McCaughey, J.H., Misson, L., Montes-Helu, M., Noormets, A., Randerson, J.T., Starr, G., Xiao, J., 2010. Ecosystem carbon dioxide fluxes after disturbance in forests of North America. J. Geophys. Res. 115, G00K02, http://dx.doi.org/10.1029/2010JG001390.

Amiro, B.D., Cantin, A., Flannigan, M.D., de Groot, W.J., 2009. Future emissions from Canadian boreal forest fires. Can. J. For. Res. 39, 383–395.

Anthoni, P.M., Unsworth, M.H., Law, B.E., Irvine, J., Baldocchi, D.D., Van Tuyl, S., Moore, D., 2002. Seasonal differences in carbon and water vapor exchange in young and old-growth ponderosa pine ecosystems. Agric. For. Meteorol. 111, 203–222.

Asner, G.P., 1998. Biophysical and biochemical sources of variability in canopy reflectance. Remote Sens. Environ. 64, 234–253.

Baldocchi, D., 2008. Breathing of the terrestrial biosphere: lessons learned from a global network of carbon dioxide flux measurement systems. Aust. J. Biotechnol. 56, 1–26.

Baldocchi, D., Falge, E., Gu, L.H., Olson, R., Hollinger, D., Running, S., Anthoni, P., Bernhofer, C., Davis, K., Evans, R., Fuentes, J., Goldstein, A., Katul, G., Law, B., Lee, X.H., Malhi, Y., Meyers, T., Munger, W., Oechel, W.U.K.T.P., Pilegaard, K., Schmid, H.P., Valentini, R., Verma, S., Vesala, T., Wilson, K., Wofsy, S., 2001. FLUXNET: a new tool to study the temporal and spatial variability of ecosystem-scale carbon dioxide, water vapor, and energy flux densities. Bull. Am. Meteorol. Soc. 82, 2415–2434.

Blackard, J.A., Finco, M.V., Helmer, E.H., Holden, G.R., Hoppus, M.L., Jacobs, D.M., Lister, A.J., Moisen, G.G., Nelson, M.D., Riemann, R., Ruefenacht, B., Salajanu, D., Weyermann, D.L., Winterberger, K.C., Brandeis, T.J., Czaplewski, R.L., McRoberts, R.E., Patterson, P.L., Tymcio, R.P., 2008. Mapping US forest biomass using nationwide forest inventory data and moderate resolution information. Remote Sens. Environ. 112, 1658–1677.

Bowman, D., Balch, J.K., Artaxo, P., Bond, W.J., Carlson, J.M., Cochrane, M.A., D'Antonio, C.M., DeFries, R.S., Doyle, J.C., Harrison, S.P., Johnston, F.H., Keeley, J.E., Krawchuk, M.A., Kull, C.A., Marston, J.B., Moritz, M.A., Prentice, I.C., Roos, C.I., Scott, A.C., Swetnam, T.W., van der Werf, G.R., Pyne, S.J., 2009. Fire in the Earth system. Science 324, 481–484.

Chambers, J.Q., Fisher, J.I., Zeng, H.C., Chapman, E.L., Baker, D.B., Hurtt, G.C., 2007. Hurricane Katrina's carbon footprint on U.S. Gulf Coast forests. Science 318, 1107.

Chapin, F.S., Matson, P.A., Vitousek, P.M., 2011. Principles of Terrestrial Ecosystem Ecology, 2nd ed. Springer, New York.

Chen, J., Chen, W.J., Liu, J., Cihlar, J., Gray, S., 2000. Annual carbon balance of Canada's forests during 1895–1996. Global Biogeochem. Cycles 14, 839–849.

Chen, J.M., Ju, W.M., Cihlar, J., Price, D., Liu, J., Chen, W.J., Pan, J.J., Black, A., Barr, A., 2003. Spatial distribution of carbon sources and sinks in Canada's forests. Tellus B: Chem. Phys. Meteorol. 55, 622–641.

Ciais, P., Reichstein, M., Viovy, N., Granier, A., Ogee, J., Allard, V., Aubinet, M., Buchmann, N., Bernhofer, C., Carrara, A., Chevallier, F., De Noblet, N., Friend, A.D., Friedlingstein, P., Grunwald, T., Heinesch, B., Keronen, P., Knohl, A., Krinner, G., Loustau, D., Manca, G., Matteucci, G., Miglietta, F., Ourcival, J.M., Papale, D., Pilegaard, K., Rambal, S., Seufert, G., Soussana, J.F., Sanz, M.J., Schulze, E.D., Vesala, T., Valentini, R., 2005. Europe-wide reduction in primary productivity caused by the heat and drought in 2003. Nature 437, 529–533.

CIFFC (Canadian Interagency Forest Fire Centre), 2014. Canada Reports by Year, http://www.ciffc.ca/ (accessed 26.02.14).

Coursolle, C., Margolis, H.A., Barr, A.G., Black, T.A., Amiro, B.D., McCaughey, J.H., Flanagan, L.B., Lafleur, P.M., Roulet, N.T., Bourque, C.P.A., Arain, M.A., Wofsy, S.C., Dunn, A., Morgenstern, K., Orchansky, A.L., Bernier, P.Y., Chen, J.M., Kidston, J., Saigusa, N., Hedstrom, N., 2006. Late-summer carbon fluxes from Canadian forests and peatlands along an east-west continental transect. Can. J. For. Res. 36, 783–800.

Davidson, E.A., Janssens, I.A., Luo, Y.Q., 2006. On the variability of respiration in terrestrial ecosystems: moving beyond Q(10). Glob. Change Biol. 12, 154–164.

Deng, F., Chen, J.M., 2011. Recent global CO_2 flux inferred from atmospheric CO_2 observations and its regional analyses. Biogeosciences 8, 3263–3281.

Deng, F., Chen, J.M., Ishizawa, M., Yuen, C.W., Mo, G., Higuchi, K., Chan, D., Maksyutov, S., 2007. Global monthly CO_2 flux inversion with a focus over North America. Tellus B: Chem. Phys. Meteorol. 59, 179–190.

Deng, F., Chen, J.M., Pan, Y., Peters, W., Birdsey, R., McCullough, K., Xiao, J., 2013. The use of forest stand age information in an atmospheric CO_2 inversion applied to North America. Biogeosciences 10, 5335–5348.

Fensholt, R., Sandholt, I., 2003. Derivation of a shortwave infrared water stress index from MODIS near- and shortwave infrared data in a semiarid environment. Remote Sens. Environ. 87, 111–121.

Field, C., Mooney, H.A., 1986. The photosynthesis–nitrogen relationship in wild plants. In: Givnish, T.J. (Ed.), Proceedings of the Sixth Maria Moors Cabot Symposium, Evolutionary Constraints on Primary Productivity: Adaptive Patterns of Energy Capture in Plants, Harvard Forest, August 1983. Cambridge Univ. Press, Cambridge, UK, pp. 25–55.

Fielder, P., Comeau, P., (Work. Pap. 53) 2000. Construction and Testing of an Inexpensive PAR Sensor Construction and Testing of an Inexpensive PAR Sensor. Res. Branch, Min. of For., Victoria, BC, Canada.

Friedl, M.A., Sulla-Menashe, D., Tan, B., Schneider, A., Ramankutty, N., Sibley, A., Huang, X.M., 2010. MODIS collection 5 global land cover: algorithm refinements and characterization of new datasets. Remote Sens. Environ. 114, 168–182.

Gao, B.C., 1996. NDWI – a normalized difference water index for remote sensing of vegetation liquid water from space. Remote Sens. Environ. 58, 257–266.

Gonsamo, A., Chen, J.M., Price, D.T., Kurz, W.A., Liu, J., Boisvenue, C., Hember, R.A., Wu, C.Y., Chang, K.H., 2013. Improved assessment of gross and net primary productivity of Canada's landmass. J. Geophys. Res. 118, 1546–1560.

Goodale, C.L., Apps, M.J., Birdsey, R.A., Field, C.B., Heath, L.S., Houghton, R.A., Jenkins, J.C., Kohlmaier, G.H., Kurz, W., Liu, S.R., Nabuurs, G.J., Nilsson, S., Shvidenko, A.Z., 2002. Forest carbon sinks in the Northern Hemisphere. Ecol. Appl. 12, 891–899.

Gurney, K.R., Law, R.M., Denning, A.S., Rayner, P.J., Baker, D., Bousquet, P., Bruhwiler, L., Chen, Y.H., Ciais, P., Fan, S., Fung, I.Y., Gloor, M., Heimann, M., Higuchi, K., John, J., Maki, T., Maksyutov, S., Masarie, K., Peylin, P., Prather, M., Pak, B.C., Randerson, J., Sarmiento, J., Taguchi, S., Takahashi, T., Yuen, C.W., 2002. Towards robust regional estimates of CO_2 sources and sinks using atmospheric transport models. Nature 415, 626–630.

Hargrove, W.W., Hoffman, F.M., Law, B.F., 2003. New analysis reveals representativeness of the AmeriFlux network. EOS 84, 529–535.

Hollinger, D.Y., Richardson, A.D., 2005. Uncertainty in eddy covariance measurements and its application to physiological models. Tree Physiol. 25, 873–885.

Houghton, R.A., Hackler, J.L., Lawrence, K.T., 1999. The US carbon budget: contributions from land-use change. Science 285, 574–578.

Huete, A., Didan, K., Miura, T., Rodriguez, E.P., Gao, X., Ferreira, L.G., 2002. Overview of the radiometric and biophysical performance of the MODIS vegetation indices. Remote Sens. Environ. 83, 195–213.

Huntzinger, D.N., Post, W.M., Wei, Y., Michalak, A.M., West, T.O., Jacobson, A.R., Baker, I.T., Chen, J.M., Davis, K.J., Hayes, D.J., Hoffman, F.M., Jain, A.K., Liu, S., McGuire, A.D., Neilson, R.P., Potter, C., Poulter, B., Price, D., Raczka, B.M., Tian, H.Q., Thornton, P., Tomelleri, E., Viovy, N., Xiao, J., Yuan, W., Zeng, N., Zhao, M., Cook, R., 2012. North American Carbon Program (NACP) regional interim synthesis: terrestrial biospheric model intercomparison. Ecol. Model. 232, 144–157.

IPCC, 2007. Climate Change 2007 – The Physical Science Basis, 2007. Contribution of Working Group I to the Fourth Assessment Report of the IPCC. Cambridge University Press, New York.

Jackson, T.J., Chen, D.Y., Cosh, M., Li, F.Q., Anderson, M., Walthall, C., Doriaswamy, P., Hunt, E.R., 2004. Vegetation water content mapping using Landsat data derived normalized difference water index for corn and soybeans. Remote Sens. Environ. 92, 475–482.

Jung, M., Reichstein, M., Bondeau, A., 2009. Towards global empirical upscaling of FLUXNET eddy covariance observations: validation of a model tree ensemble approach using a biosphere model. Biogeosciences 6, 2001–2013.

Kennedy, R.E., Yang, Z.G., Cohen, W.B., 2010. Detecting trends in forest disturbance and recovery using yearly Landsat time series: 1. LandTrendr – temporal segmentation algorithms. Remote Sens. Environ. 114, 2897–2910.

Knyazikhin, Y., Schull, M.A., Stenberg, P., Mottus, M., Rautiainen, M., Yang, Y., Marshak, A., Carmona, P.L., Kaufmann, R.K., Lewis, P., Disney, M.I., Vanderbilt, V., Davis, A.B., Baret, F., Jacquemoud, S., Lyapustin, A., Myneni, R.B., 2013. Hyperspectral remote sensing of foliar nitrogen content. Proc. Natl. Acad. Sci. U. S. A. 110, E185–E192.

Kurz, W.A., Apps, M.J., 1999. A 70-year retrospective analysis of carbon fluxes in the Canadian forest sector. Ecol. Appl. 9, 526–547.

Kurz, W.A., Dymond, C.C., Stinson, G., Rampley, G.J., Neilson, E.T., Carroll, A.L., Ebata, T., Safranyik, L., 2008. Mountain pine beetle and forest carbon feedback to climate change. Nature 452, 987–990.

LeBauer, D.S., Treseder, K.K., 2008. Nitrogen limitation of net primary productivity in terrestrial ecosystems is globally distributed. Ecology 89, 371–379.

Lindroth, A., Lagergren, F., Grelle, A., Klemedtsson, L., Langvall, O., Weslien, P., Tuulik, J., 2009. Storms can cause Europe-wide reduction in forest carbon sink. Glob. Change Biol. 15, 346–355.

Liu, S.G., Bond-Lamberty, B., Hicke, J.A., Vargas, R., Zhao, S.Q., Chen, J., Edburg, S.L., Hu, Y.M., Liu, J.X., McGuire, A.D., Xiao, J.F., Keane, R., Yuan, W.P., Tang, J.W., Luo, Y.Q., Potter, C., Oeding, J., 2011. Simulating the impacts of disturbances on forest carbon cycling in North America: processes, data, models, and challenges. J. Geophys. Res. 116, G00K08, http://dx.doi.org/10.1029/2010JG001585.

Lloyd, J., Taylor, J.A., 1994. On the temperature-dependence of soil respiration. Funct. Ecol. 8, 315–323.

Loescher, H.W., Law, B.E., Mahrt, L., Hollinger, D.Y., Campbell, J., Wofsy, S.C., 2006. Uncertainties in, and interpretation of, carbon flux estimates using the eddy covariance technique. J. Geophys. Res. 111, D21S90, http://dx.doi.org/10.1029/2005JD006932.

Magnani, F., Mencuccini, M., Borghetti, M., Berbigier, P., Berninger, F., Delzon, S., Grelle, A., Hari, P., Jarvis, P.G., Kolari, P., Kowalski, A.S., Lankreijer, H., Law, B.E., Lindroth, A., Loustau, D., Manca, G., Moncrieff, J.B., Rayment, M., Tedeschi, V., Valentini, R., Grace, J., 2007. The human footprint in the carbon cycle of temperate and boreal forests. Nature 447, 848–850.

Masek, J.G., Goward, S.N., Kennedy, R.E., Cohen, W.B., Moisen, G.G., Schleeweis, K., Huang, C.Q., 2013. United States forest disturbance trends observed using Landsat time series. Ecosystems 16, 1087–1104.

McCarthy, H.R., Oren, R., Kim, H.S., Johnsen, K.H., Maier, C., Pritchard, S.G., Davis, M.A., 2006. Interaction of ice storms and management practices on current carbon sequestration in forests with potential mitigation under future CO_2 atmosphere. J. Geophys. Res. 111, D15103, http://dx.doi.org/10.1029/2005JD006428.

Mesinger, F., DiMego, G., Kalnay, E., Mitchell, K., Shafran, P.C., Ebisuzaki, W., Jovic, D., Woollen, J., Rogers, E., Berbery, E.H., Ek, M.B., Fan, Y., Grumbine, R., Higgins, W., Li, H., Lin, Y., Manikin, G., Parrish, D., Shi, W., 2006. North American regional reanalysis. Bull. Am. Meteorol. Soc. 87, 343–360.

Moffat, A.M., Papale, D., Reichstein, M., Hollinger, D.Y., Richardson, A.D., Barr, A.G., Beckstein, C., Braswell, B.H., Churkina, G., Desai, A.R., Falge, E., Gove, J.H., Heimann, M., Hui, D.F., Jarvis, A.J., Kattge, J., Noormets, A., Stauch, V.J., 2007. Comprehensive comparison of gap-filling techniques for eddy covariance net carbon fluxes. Agric. For. Meteorol. 147, 209–232.

Nemani, R., White, M., Thornton, P., Nishida, K., Reddy, S., Jenkins, J., Running, S., 2002. Recent trends in hydrologic balance have enhanced the terrestrial carbon sink in the United States. Geophys. Res. Lett. 29, http://dx.doi.org/10.1029/2002GL014867.

Ollinger, S.V., Richardson, A.D., Martin, M.E., Hollinger, D.Y., Frolking, S.E., Reich, P.B., Plourde, L.C., Katul, G.G., Munger, J.W., Oren, R., Smithb, M.L.U.K.T.P., Bolstad, P.V., Cook, B.D., Day, M.C., Martin, T.A., Monson, R.K., Schmid, H.P., 2008. Canopy nitrogen, carbon assimilation, and albedo in temperate and boreal forests: functional relations and potential climate feedbacks. Proc. Natl. Acad. Sci. U. S. A. 105, 19336–19341.

Oren, R., Ellsworth, D.S., Johnsen, K.H., Phillips, N., Ewers, B.E., Maier, C., Schafer, K.V.R., McCarthy, H., Hendrey, G., McNulty, S.G., Katul, G.G., 2001. Soil fertility limits carbon sequestration by forest ecosystems in a CO_2-enriched atmosphere. Nature 411, 469–472.

Pacala, S.W., Hurtt, G.C., Baker, D., Peylin, P., Houghton, R.A., Birdsey, R.A., Heath, L., Sundquist, E.T., Stallard, R.F., Ciais, P., Moorcroft, P., Caspersen, J.P., Shevliakova, E., Moore, B., Kohlmaier, G., Holland, E., Gloor, M., Harmon, M.E., Fan, S.M., Sarmiento, J.L., Goodale, C.L., Schimel, D., Field, C.B., 2001. Consistent land- and atmosphere-based US carbon sink estimates. Science 292, 2316–2320.

Palmer, W.C., 1965. Meteorological Drought, Research Paper No. 45. U.S. Department of Commerce, Washington DC.

Pan, Y.D., Birdsey, R.A., Fang, J.Y., Houghton, R., Kauppi, P.E., Kurz, W.A., Phillips, O.L., Shvidenko, A., Lewis, S.L., Canadell, J.G., Ciais, P., Jackson, R.B., Pacala, S.W., McGuire, A.D., Piao, S.L., Rautiainen, A., Sitch, S., Hayes, D., 2011a. A large and persistent carbon sink in the world's forests. Science 333, 988–993.

Pan, Y.D., Chen, J.M., Birdsey, R., McCullough, K., He, L., Deng, F., 2011b. Age structure and disturbance legacy of North American forests. Biogeosciences 8, 715–732.

Peichl, M., Brodeur, J.J., Khomik, M., Arain, M.A., 2010. Biometric and eddy-covariance based estimates of carbon fluxes in an age-sequence of temperate pine forests. Agric. For. Meteorol. 150, 952–965.

Raczka, B.M., Davis, K.J., Huntzinger, D., Neilson, R.P., Poulter, B., Richardson, A.D., Xiao, J.F., Baker, I., Ciais, P., Keenan, T.F., Law, B., Post, W.M., Ricciuto, D., Schaefer, K., Tian, H.Q., Tomelleri, E., Verbeeck, H., Viovy, N., 2013. Evaluation of continental carbon cycle simulations with North American flux tower observations. Ecol. Monogr. 83, 531–556.

Reich, P.B., Hungate, B.A., Luo, Y.Q., 2006. Carbon–nitrogen interactions in terrestrial ecosystems in response to rising atmospheric carbon dioxide. Annu. Rev. Ecol. Evol. Syst. 37, 611–636.

RuleQuest, 2008. http://www.rulequest.com (visited on 10/18/07).

Ryu, Y., Baldocchi, D.D., Kobayashi, H., van Ingen, C., Li, J., Black, T.A., Beringer, J., van Gorsel, E., Knohl, A., Law, B.E., Roupsard, O., 2011. Integration of MODIS land and atmosphere products with a coupled-process model to estimate gross primary productivity and evapotranspiration from 1 km to global scales. Global Biogeochem. Cycles 25, http://dx.doi.org/10.1029/2011GB004053.

Schaaf, C.B., Gao, F., Strahler, A.H., Lucht, W., Li, X.W., Tsang, T., Strugnell, N.C., Zhang, X.Y., Jin, Y.F., Muller, J.P., Lewis, P., Barnsley, M., Hobson, P., Disney, M., Roberts, G., Dunderdale, M., Doll, C., d'Entremont, R.P., Hu, B.X., Liang, S.L., Privette, J.L., Roy, D., 2002. First operational BRDF, albedo nadir reflectance products from MODIS. Remote Sens. Environ. 83, 135–148.

Schimel, D., Melillo, J., Tian, H.Q., McGuire, A.D., Kicklighter, D., Kittel, T., Rosenbloom, N., Running, S., Thornton, P., Ojima, D., Parton, W., Kelly, R., Sykes, M., Neilson, R., Rizzo, B., 2000. Contribution of increasing CO_2 and climate to carbon storage by ecosystems in the United States. Science 287, 2004–2006.

Schmidt, A., Hanson, C., Chan, W.S., Law, B.E., 2012. Empirical assessment of uncertainties of meteorological parameters and turbulent fluxes in the AmeriFlux network. J. Geophys. Res. 117, G04014, http://dx.doi.org/10.1029/2012JG002100.

Schwalm, C.R., Williams, C.A., Schaefer, K., Arneth, A., Bonal, D., Buchmann, N., Chen, J.Q., Law, B.E., Lindroth, A., Luyssaert, S., Reichstein, M., Richardson, A.D., 2010. Assimilation exceeds respiration sensitivity to drought. A FLUXNET synthesis. Glob. Change Biol. 16, 657–670.

Snaydon, R.W., 1991. The productivity of C3 and C4 plants – a reassessment. Funct. Ecol. 5, 321–330.

SOCCR, 2007. In: Dilling, L, King, A.W., Zimmerman, G.P., Fairman, D.M., Houghton, R.A., Marland, G.A., Rose, A.Z., Wilbanks, T.J. (Eds.), The First State of the Carbon Cycle Report (SOCCR). The North American Carbon Budget and Implications for the Global Carbon Cycle. , p. 264.

Stocks, B.J., Mason, J.A., Todd, J.B., Bosch, E.M., Wotton, B.M., Amiro, B.D., Flannigan, M.D., Hirsch, K.G., Logan, K.A., Martell, D.L., Skinner, W.R., 2002. Large forest fires in Canada, 1959–1997. J. Geophys. Res. 108, http://dx.doi.org/10.1029/2001JD000484, NO. D1, 8149.

Sun, G., Caldwell, P., Noormets, A., McNulty, S.G., Cohen, E., Myers, J.M., Domec, J.C., Treasure, E., Mu, Q.Z., Xiao, J.F., John, R., Chen, J.Q., 2011. Upscaling key ecosystem functions across the conterminous United States by a water-centric ecosystem model. J. Geophys. Res. 116, G00J05, http://dx.doi.org/10.1029/2010JG001573.

Townsend, P.A., Serbin, S.P., Kruger, E.L., Gamon, J.A., 2013. Disentangling the contribution of biological and physical properties of leaves and canopies in imaging spectroscopy data. Proc. Natl. Acad. Sci. U. S. A. 110, E1074.

Verbeeck, H., Samson, R., Verdonck, F., Lemeur, R., 2006. Parameter sensitivity and uncertainty of the forest carbon flux model FORUG: a Monte Carlo analysis. Tree Physiol. 26, 807–817.

Wan, Z.M., Zhang, Y.L., Zhang, Q.C., Li, Z.L., 2002. Validation of the land-surface temperature products retrieved from terra moderate resolution imaging spectroradiometer data. Remote Sens. Environ. 83, 163–180.

Wang, W.L., Dungan, J., Hashimoto, H., Michaelis, A.R., Milesi, C., Ichii, K., Nemani, R.R., 2011. Diagnosing and assessing uncertainties of terrestrial ecosystem models in a multimodel ensemble experiment: 2. Carbon balance. Glob. Change Biol. 17, 1367–1378.

Waring, R.H., Franklin, J.F., 1979. Evergreen coniferous forests of the Pacific Northwest. Science 204, 1380–1386.

Wiedinmyer, C., Neff, J.C., 2007. Estimates of CO_2 from fires in the United States: implications for carbon management. Carbon Balance Manage. 2, http://dx.doi.org/10.1186/1750-0680-2-10.

Wright, I.J., Reich, P.B., Cornelissen, J.H.C., Falster, D.S., Garnier, E., Hikosaka, K., Lamont, B.B., Lee, W., Oleksyn, J., Osada, N., Poorter, H., Villar, R., Warton, D.I., Westoby, M., 2005. Assessing the generality of global leaf trait relationships. New Phytol. 166, 485–496.

Xiao, J.F., Chen, J.Q., Davis, K.J., Reichstein, M., 2012. Advances in upscaling of eddy covariance measurements of carbon and water fluxes. J. Geophys. Res. 117, G00J01, http://dx.doi.org/10.1029/2011JG001889.

Xiao, J.F., Davis, K.J., Urban, N.M., Keller, K., 2014. Uncertainty in model parameters and regional carbon fluxes: a model-data fusion approach. Agric. For. Meteorol. 189, 175–186.

Xiao, J.F., Davis, K.J., Urban, N.M., Keller, K., Saliendra, N.Z., 2011b. Upscaling carbon fluxes from towers to the regional scale: influence of parameter variability and land cover representation on regional flux estimates. J. Geophys. Res. 116, G00J06, http://dx.doi.org/10.1029/2010JG001568.

Xiao, J.F., Moody, A., 2004. Photosynthetic activity of US biomes: responses to the spatial variability and seasonality of precipitation and temperature. Glob. Change Biol. 10, 437–451.

Xiao, J.F., Zhuang, Q.L., Baldocchi, D.D., Law, B.E., Richardson, A.D., Chen, J.Q., Oren, R., Starr, G., Noormets, A., Ma, S.Y., Verma, S.B., Wharton, S., Wofsy, S.C., Bolstad, P.V., Burns, S.P., Cook, D.R., Curtis, P.S., Drake, B.G., Falk, M., Fischer, M.L., Foster, D.R., Gu, L.H., Hadley, J.L., Hollinger, D.Y., Katul, G.G., Litvak, M., Martin, T.A., Matamala, R., McNulty, S., Meyers, T.P., Monson, R.K., Munger, J.W., Oechel, W.C., Paw U, K.T., Schmid, H.P., Scott, R.L., Sun, G., Suyker, A.E., Torn, M.S., 2008. Estimation of net ecosystem carbon exchange for the conterminous United States by combining MODIS and AmeriFlux data. Agric. For. Meteorol. 148, 1827–1847.

Xiao, J.F., Zhuang, Q.L., Law, B.E., Baldocchi, D.D., Chen, J.Q., Richardson, A.D., Melillo, J.M., Davis, K.J., Hollinger, D.Y., Wharton, S., Oren, R., Noormets, A., Fischer, M.L., Verma, S.B., Cook, D.R., Sun, G., McNulty, S., Wofsy, S.C., Bolstad, P.V., Burns, S.P., Curtis, P.S., Drake, B.G., Falk, M., Foster, D.R., Gu, L.H., Hadley, J.L., Katulk, G.G., Litvak, M., Ma, S.Y., Martinz, T.A., Matamala, R., Meyers, T.P., Monson, R.K., Munger, J.W., Oechel, W.C., Paw U, K.T., Schmid, H.P., Scott, R.L., Starr, G., Suyker, A.E., Torn, M.S., 2011a. Assessing net ecosystem carbon exchange of U.S. terrestrial ecosystems by integrating eddy covariance flux measurements and satellite observations. Agric. For. Meteorol. 151, 60–69.

Xiao, J.F., Zhuang, Q.L., Law, B.E., Chen, J.Q., Baldocchi, D.D., Cook, D.R., Oren, R., Richardson, A.D., Wharton, S., Ma, S.Y., Martin, T.A., Verma, S.B., Suyker, A.E., Scott, R.L., Monson, R.K., Litvak, M., Hollinger, D.Y., Sun, G., Davis, K.J., Bolstad, P.V., Burns, S.P., Curtis, P.S., Drake, B.G., Falk, M., Fischer, M.L., Foster, D.R., Gu, L.H., Hadley, J.L., Katul, G.G., Roser, Y., McNulty, S., Meyers, T.P., Munger, J.W., Noormets, A., Oechel, W.C., Paw, K.T., Schmid, H.P., Starr, G., Torn, M.S., Wofsy, S.C., 2010. A continuous measure of gross primary production for the conterminous United States derived from MODIS and AmeriFlux data. Remote Sens. Environ. 114, 576–591.

Xiao, J.F., Zhuang, Q.L., Liang, E.Y., McGuire, A.D., Moody, A., Kicklighter, D.W., Shao, X.M., Melillo, J.M., 2009. Twentieth-century droughts and their impacts on terrestrial carbon cycling in China. Earth Interact. 010, 1–31, http://dx.doi.org/10.1175/2009EI275.1.

Zhang, K., Kimball, J.S., Zhao, M.S., Oechel, W.C., Cassano, J., Running, S.W., 2007. Sensitivity of pan-Arctic terrestrial net primary productivity simulations to daily surface meteorology from NCEP-NCAR and ERA-40 reanalyses. J. Geophys. Res. 112, G01011, http://dx.doi.org/10.1029/2006JG000249.

Zhang, L., Guo, H.D., Jia, G.S., Wylie, B., Gilmanov, T., Howard, D., Ji, L., Xiao, J.F., Li, J., Yuan, W.P., Zhao, T.B., Chen, S.P., Zhou, G.S., Kato, T., 2014. Net ecosystem productivity of temperate grasslands in northern China: an upscaling study. Agric. For. Meteorol. 184, 71–81.

Zhang, X.Y., Kondragunta, S., 2006. Estimating forest biomass in the USA using generalized allometric models and MODIS land products. Geophys. Res. Lett. 33, L09402, http://dx.doi.org/10.1029/2006GL025879.

Zhao, M.S., Running, S.W., 2010. Drought-induced reduction in global terrestrial net primary production from 2000 through 2009. Science 329, 940–943.